Characterization of Polyphenoxyethylphenoxyphosphazene - Bulk Sealant Applications

by
C. A. Williams

Thesis submitted to the faculty of Virginia Polytechnic and State University in partial fulfillment of the requirements for the degree of

Master of Science

in

Chemistry

APPROVED

T. C. Ward, Chairman

J. P. Wightman

J. G. Dillard

c.2

LD
3655
V855
1995
W555
c.2

CHARACTERIZATION OF POLYPHENOXY-ETHYLPHENOXYPHOSPHAZENE - BULK SEALANT APPLICATIONS

by

Carl A. Williams

Dr. T. C. Ward, Chairman

Chemistry

Polymer chemistry has primarily been a main chain carbon-based science, but recently the usage of inorganic polymeric materials has increased with polyphosphazene research leading the way. The credit for the increased interest in the field of phosphazene chemistry arises from the unique physical properties these materials possess. Depending upon the rigidity of the side group, the morphology of these materials is controllable. A high degree of chain mobility is exhibited by this class of polymers resulting in low glass transitions. The industrial applications of these materials are quite divergent as a result of the various morphologies and glass transitions. Possible sealant applications of these materials are apparent and have yet to be realized. These will be the focus of this thesis.

The objective of this research was to characterize polyphenoxy-ethylphenoxyphosphazene in terms of three bulk properties to determine the possibility of favorable sealant application. Investigation of the solubility parameter through solvent ingression experiments determined

the solvent resistive abilities of the material. Thermogravimetric analysis set an upper temperature limit of application by determining the thermal stability of the polymer. The study of polyphenoxy-ethylphenoxy-phospazene through dynamic mechanical analysis provided insight into the vibrational damping characteristics of the material as well as establishing a lower temperature limit of possible use. Combination of the results from these various experiments enables one to make qualitative conclusions regarding favorable sealant application.

Acknowledgments

The author would like to thank the following people and organizations for their support and guidance during the completion of this work.

To my wife **Kristi** and son **Maxwell** your patience and understanding during the good times and bad carried me through. Without your encouragment and confidence in me I most likely would not have completed this advanced degree. **Kristi,** thank you for the long days and nights spent in the editing, we make a great team.

To my mother **Sondra** and father **John** who provided me with the opportunity to attend college. Their love and support have always been a mainstay in my life and without it I would not have come this far.

To my sister **Jill**, keep the faith and thanks.

To the **Lilly family**, much love and thanks.

To **Dr. Ward and family**, thank you for taking me in and treating me as one of your own. **Dr. Ward,** you provided me the opportunity to expand my mind when you took me on as an undergraduate researcher many years ago. Your confidence in my ability to attend graduate school (even though I had my doubts) was one of the driving forces towards graduation and was always in the back of my mind. You are an exceptional teacher and good friend whom I shall never forget.

To **Drs. Dillard and Wightman**, many thanks for being members of my committee. The time I spent in your classes was enjoyable and I shall always have fond memories of my years at Virginia Tech.

To the members of **Polypkem**, old and new, the assistance that each of you provided during the completion of this project was invaluable. Our many conversations in the lab and other places (i.e. VTGC, Champs ...) were always interesting and I will remember each of you as good freinds.

To the **National Science Foundation** and **Center for Adhesive and Sealant Sciences** for their monetary support of this work.

Table of Contents

		Pages
LITERATURE REVIEW (1 - 5)		
1	INTRODUCTION	1
2.	POLYPHOSPHAZENES	3
2.1	BACKGROUND	3
2.2	SYNTHESIS	4
2.3	PHYSICAL PROPERTIES	9
2.3.1	STRUCTURE	9
2.3.2	THERMAL PROPERTIES	12
2.3.4	THERMAL STABILITY	14
2.3.5	SOLUTION BEHAVIOR	19
2.3.6	MECHANICAL PROPERTIES	21
3.0	SOLUBILITY PARAMETER (δ)	24
3.1	ESTIMATION OF δ	25
3.2	EXPERIMENTAL DETERMINATION OF δ	26
4.0	MECHANICAL PROPERTIES	29
4.1	THEORY	30
4.2	RELAXATIONS	32
5.0	THERMAL ANALYSIS	35
5.1	THERMOGRAVIMETRIC ANALYSIS	35
6.0	EXPERIMENTAL	39
6.1	MATERIALS	39
6.2	SOLUTION PROPERTIES	40
6.3	THERMAL STABILITY	41
6.4	DYNAMIC MECHANICAL EVALUATION	41

7.0 RESULTS AND DISCUSSIONS 43
7.1 SOLUTION PROPERTIES 43
7.1.1 ESTIMATION OF δ 43
7.1.2 SOLUBILITY INVESTIGATION 46
7.2 THERMAL STABILITY 54
7.3 DYNAMIC MECHANICAL EVALUATION 60

8 CONCLUSIONS 6

9 REFERENCES 70

10 ACKNOWLEDGMENTS 72

List of Figures and Tables

Figure or Table		Pages
Figure 1.	Typical Repeat Unit of Polyphosphazenes	2
Scheme 1.	Reaction Pathway for Hexachlorocyclotriphosphazene	4
Scheme 2.	Reaction Pathway for Polydichlorophosphazene	6
Table 1.	Various Classes of Polyphosphazenes	8
Figure 2.	Representation of Orbital Mismatch in Bonding	11
Table 2.	Thermal Transitions in Selected Polyphosphazenes	13
Table 3.	Thermal Stability in Selected Polyphosphazenes	14
Scheme 3.	Crosslinking Reaction Mechanism of Cyclic Species	18
Table 4.	Activation Energies of α Transitions	23
Table 5.	Solubility Relationships	25
Figure 3.	Typical Dynamic Mechanical Spectra	32
Figure 4.	Repeat Unit for Polyphenoxy-ethylphenoxyphosphazene	39
Table 6.	Additive equations for Solubility Parameter	43
Table 7.	Estimation of Solubility Parameter	44
Table 8.	Solvents Used in Solvent Ingression Study	46
Table 9.	Weight Gain in Various Solvents	47
Figure 5.	Percent Weight Gain vs Time	48
Figure 6.	Percent Weight Gain vs Solubility Parameter	49
Figure 7.	Two Dimensional Representation of Solubility Parameters	50
Figure 8.	Effect of Individual Solubility Parameter Component	52
Figure 9.	Thermal Profile in Air and Nitrogen Atmospheres	54
Figure 10.	Isoconversional Plot in Nitrogen	57
Table 10.	Calculated Activation Energies in Nitrogen	58
Figure 11.	Isoconversional Plot in Air	59
Figure 12.	Dynamic Mechanical Spectra of Polyaryloxyphosphazene	61
Figure 13.	Scanning Electron Micrographs of Polyaryloxyphosphazene	63
Figure 14.	Differential Scanning Calorimetry Profile	64
Figure 15.	Multi-Frequency Spectra of Polyaryloxyphosphazene	65
Figure 16.	Activation Energies for α Transitions	67

1.0 Introduction

The field of polymer chemistry has developed largely around the study of materials composed of main chain organic molecules. Recent interest in experimenting with new combinations of materials has highlighted the importance of inorganic polymeric materials. Polyphosphazene research leads the way.

The polyphosphazene repeat unit consists of alternating phosphorus and nitrogen atoms connected by successive single and double bonds. Phosphorus is bonded with two substituents and Figure 1 depicts the typical repeat unit of polyorganophosphazenes, where the symbol R represents a wide variety of substituents. The effect of these substituential variations will be discussed later. Increased interest in these compounds resulted in the development of over 300 stable phosphazene polymers and this number is ever increasing.

Because of the unique physical properties these materials possess there has been rapid progress in the field of polyphosphazene chemistry. The high degree of chain mobility these polymers display allows their morphology to be controlled as a function of the substituents' rigidity.[1-2] Polyphosphazenes' ability to resist photolytic and oxidative degradation provides high temperature stability and flame retardent properties. The industrial applications of these materials are extensive, resulting from the variable morphologies that are obtainable.[3] The focus of this thesis is to

determine the possibilities for sealant applications of these materials, that have not yet been completely realized.

Use of solution, thermal, and dynamic mechanical experiments allow one to investigate possible sealant applications of polyphenoxy-ethylphenoxyphosphazene. Solution studies determine the solvent resistive abilities of the material. Thermal experiments establish the thermal stability of the material and set an upper temperature limit of usage. Dynamic mechanical investigations determine the vibrational damping capabilities of the material and establish a lower temperature limit of application.

Figure 1. Repeat unit of a polyphosphazene where R and R' represent a wide variety of substituents

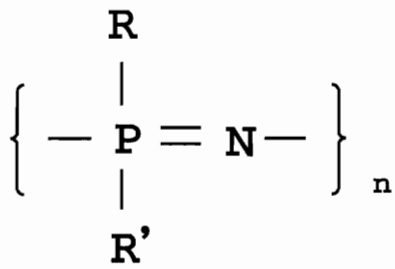

Literature Search

2.0 Polyphosphazenes

2.1 Background

Phosphazene chemistry originated in 1834 when Wolher[4] and Rose[5] showed that phosphorus pentachloride reacts with ammonia to form a crystalline white solid, $(NPCl_2)_3$, later named hexachlorocyclotri-phosphazene. Scheme 1 depicts this reaction pathway. These early explorations received little attention until the late 1890's when Stokes[6] identified the existence of cyclic species up to $(NPCl_2)_7$. Stokes found that the application of heat transformed these cyclic chlorophosphazenes into elastic materials that became commonly known as inorganic rubber. Additional heating of this new elastomeric material decomposed it to the cyclic components. However, this new compound's insolubility, resulting from its crosslinked structure slowed further investigation.

During the 1960's Allcock and Kugel[7] developed a method by which hexachlorocyclotriphospazene was polymerized without the formation of the crosslinked material. The scientists found that through control of reaction time, temperature, and purity of the trimer, they formed a linear polymer that was soluble in most organic solvents. Besides synthesizing an uncrosslinked species, the formation of organophosphazene compounds became possible due to the reactivity of the P-Cl bonds.

Continued heating resulted in the formation of an insoluble rubber, just as Stokes had discovered some 60 years earlier. This early research catapulted polyphospazene chemistry into one of the most popular fields of inorganic polymer chemistry to date.

Scheme 1. Preparation of Hexachlorocyclotriphosphazene

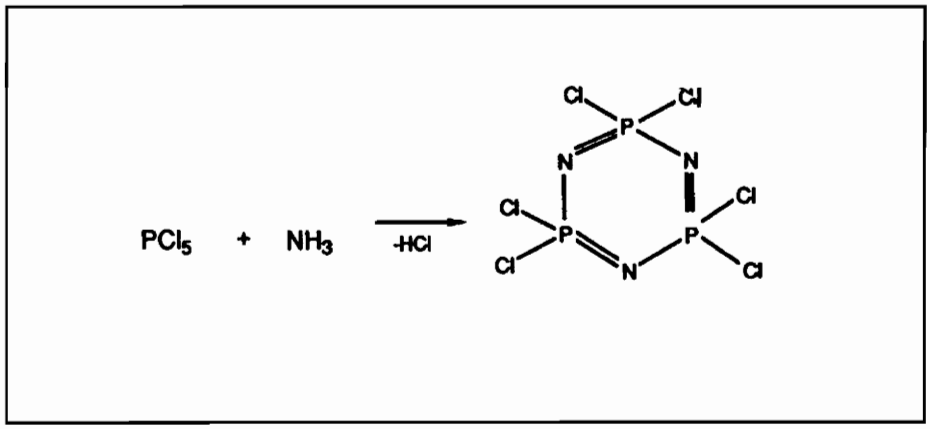

2.2 Synthesis

The intricacies involved in the synthesis of polyorganophosphazenes is extensive and control of the variables is critical to the formation of completely substituted materials. The formation of polyorgano-phosphazenes occurs through macromolecular substitution of a reactive

intermediate, polydichlorophosphazene. The development of the reactive intermediate has received a considerable amount of attention and some of the more common methods used in its formation are discussed.

Allcock and others have reported the formation of linear dichlorophosphazene through a combination of phosphorus pentachloride and ammonia. On completion of the formation of hexachlorocyclotriphospazene, polymerization occurs by increasing the reaction temperature to 250°C and applying a vacuum. Further research conducted by Hornbaker and Li[8] showed that polydichlorophosphazene polymerizes from phosphorus pentachloride and ammonium chloride, bypassing the formation of hexachlorocylophosphazene. Heloui and others[9] further refined the preparation of the intermediate by performing a condensation reaction using N-dichlorophosphoryl-p-trichloromonophosphazene. The elimination of phosphoryl chloride results in the desired product while providing improved molecular weight control through the addition of a chain limiter or careful control of reaction time. Scheme 2 illustrates all of these reaction pathways.

The macromolecular substitution of polydichlorophosphazene has been performed using a wide variety of organic nucleophiles. The uncrosslinked polydichlorophosphazene is initially dissolved in an inert solvent and then added dropwise to a solution containing the desired nucleophile. As the substitution progresses, the polymer and salt precipates out of the solution. The reaction time, temperature, and solvent mixtures are all dependent upon the reactivity of the nucleophile[10].

The synthesis of polyalklyoxyphosphazenes occurs in solvent mixtures of benzene and tetrahydrofuran to dissolve the two compounds. While using reaction temperatures of 60-80°C, dropwise addition of the

solvated intermediate to excessive amounts of sodium alkyloxides results in percent yields ranging from 60 to 80% .[11]

Scheme 2. Reaction pathways for Polydichlorophosphazene

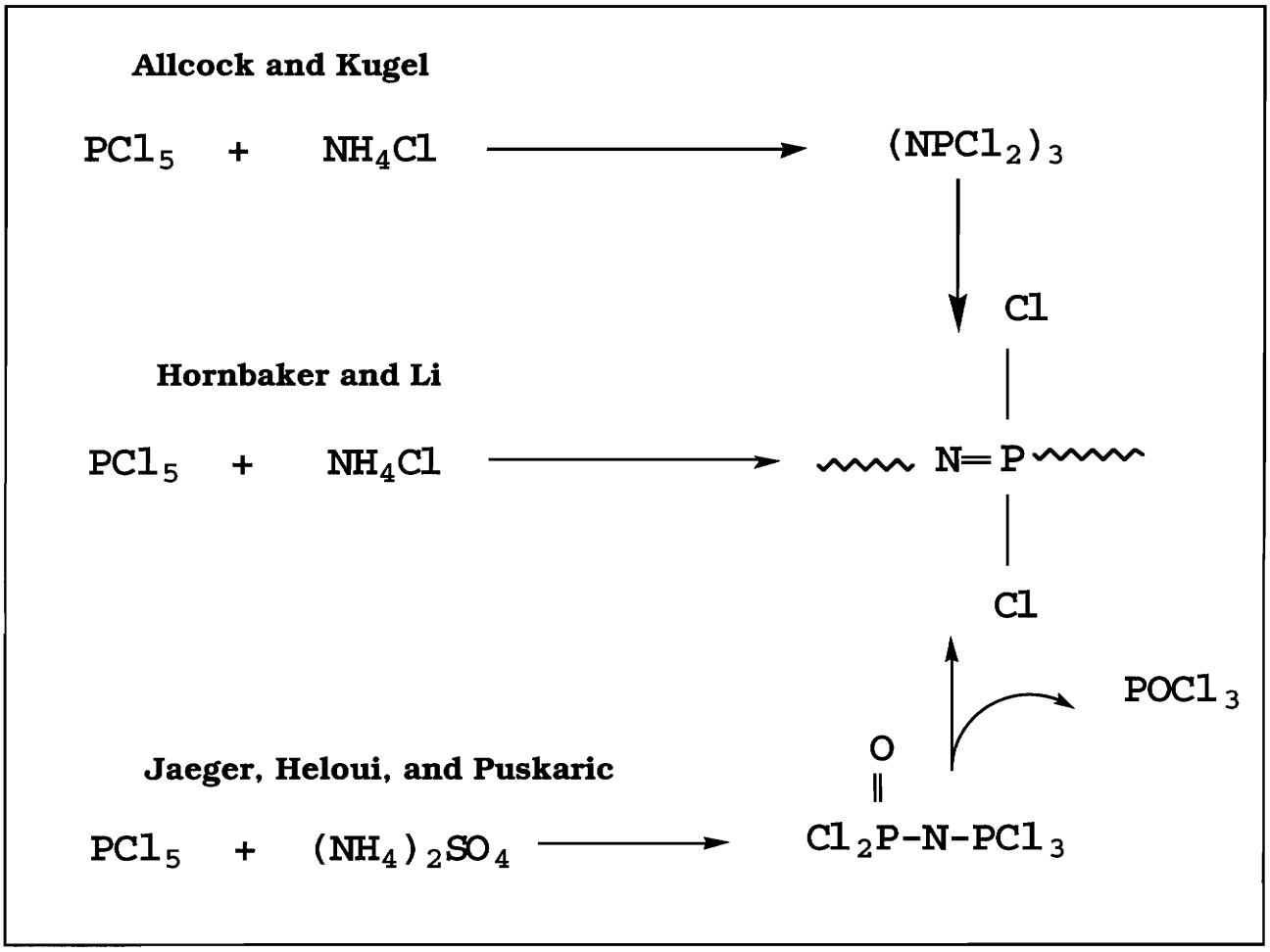

The decreased reactivity of sodium aryloxyides results in increased reaction temperatures. The synthesis of polyaryloxyphosphazenes occurs at 115 - 125°C when solution mixtures of toluene and diglyme have

dissolved the intermediate and nucleophile. Dropwise addition of the intermediate solution to the nucleophile results in 30 to 80 percent yields.[12] Solvent mixtures of benzene and tetrahydrofuran decrease the reaction temperature but unstable polymers result due to incomplete substitution.[13]

The conditions used in the formation of polyaminophosphazenes are similar to those used in the polymerization of polyakyloxyphosphazenes. To eliminate the formation of crosslinked products when attempting to react nucleophilic primary amines and ammonia substituents, reduction of reaction temperatures and times is vital.[14] Table 1 shows some representative compositions for the various classes of polyphosphazenes discussed above.

Complications arise when attempting substitution reactions with organometallic compounds and polydichlorophosphazene. The addition of these metallic nucleophiles results in the depolymerization and subsequent cleavage of the P-N bonds. Replacing the chlorine substituents with fluorine atoms allows the reaction to progress without significant degradation.[15] The P-C bond that results from this reaction provides excellent thermal stability when compared with other polyorganophosphazenes.

Several researchers have considered alternate forms of polymerization but found them less successful than the techniques set forth above. Allcock and Evans have shown that substitution of hexachlorocyclotriphosphazene with a single organic group and carrying out a ring opening polymerization results in the formation of the product but with decreased percent yields.[16] Others have attempted direct

synthetic techniques to form polyorganophosphazenes that previously were unattainable through the nucleophilic substitution methods.

Table 1. Various classes of Polyphosphazenes

- Polyalkyoxyphosphazenes
  $\{(CH_3O)_2PN\}_n$
  $\{(CF_3CH_2O)_2PN\}_n$
  $\{(CF_3CH_2O)(CF_3CF_2CF_2CH_2O)PN\}_n$

- Polyaryloxyphosphazenes
  $\{(C_6H_5O)_2PN\}_n$
  $\{(p\text{-}C_6H_5C_6H_4O)_2PN\}_n$
  $\{(m\text{-}CH_3C_6H_4O)_2PN\}_n$

- Polyaminophosphazenes
  $\{(CH_3NH)_2PN\}_n$
  $\{(C_6H_5NH)_2PN\}_n$

Pyrolysis of silylphosphinimines has been the primary method used to form these new structures, but few researchers are pursuing this technique further. [17]

2.3 Physical Properties

Interest in polyphosphazene chemistry is associated with the unique physical characteristics that these materials display and the wide variety of substituents the polymer chain can support. Over the last 30 years researchers have identified and documented the physical characteristics of polyphosphazenes. They have focused on the structure, thermal transitions and stability, solution behavior, and dynamic mechanical response. These are outlined below.

2.3.1 Structure

The outward appearance of the polyphosphazene structure would lead one to conclude that these materials exist as rigid semicrystalline polymers. Polyphosphazenes can possess a variety of morphologies and demonstrate variable thermal and solvent stability. However, the one characteristic consistent to all polyphosphazenes is backbone flexibility.

The skeletal backbone consists of alternating single and double bonds between phosphorus and nitrogen atoms, which do not behave in a manner analogous to classical open ended conjugated carbon based

systems. Both phosphorus and nitrogen possess five valence electrons for use in bond formation. Phosphorus donates four electrons while nitrogen donates two electrons and a single lone pair of electrons to the formation of the sigma bonds. The nonbonding electrons, one for each molecule, inhabit the $2p_z$ orbital on nitrogen and the 3d orbital on phosphorous. These electrons combine to form a restrained localized p_π - d_π bond. As a consequence of the orbital mismatch that occurs on each phosphorous, a three centered island π-bonding effect arises. Figure 2 illustrates this bonding phenomenon. Because phosphorus possesses five 3d orbitals, rotation of the P - N bond allows the p-orbital of nitrogen to project upon any of the d-orbitals of phosphorus.[18] This results in much smaller rotational barriers for polyphosphazenes than typical p_π-d_π double bonds found in most organic compounds. The barrier to rotation that phosphorous - nitrogen bonds exhibit is 3.38 kJ/mol and 21.8 kJ/mol for polydifluorethoxy- and polydiphenoxyphosphazene, respectively.[19]

Another factor influencing the physical properties of polyphosphazenes is chain conformation. The torsional angles of the bonded polymer backbone influence the shape of a polymer's chain. These acquired angles depend upon two factors: (1) repulsion or attractions of neighboring substituents on the chain and (2) intramolecular forces associated with the packing of molecules into possible micro - crystalline formations.[18] Polyphosphazenes are separated from most other carbon based systems, because the side groups are bonded to every other

Figure 2 Drawing illustrating the hybridization of the phosphorous 3d orbitals and the nitrogen $2p_z$ orbitals. A discontinuity in the overlap of the orbitals is clearly apparent in this representation.

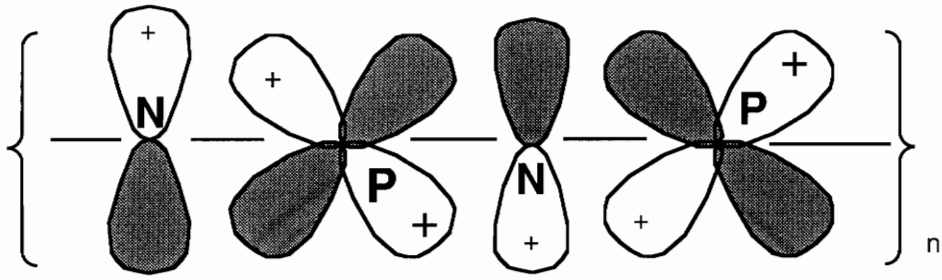

skeletal atom. Therefore the attraction or repulsion of the substituents effects the chain conformation of polyphosphazenes. The cis-trans chain structure allows for the largest degree of space between the substituents, thereby minimizing the intramolecular forces between the side groups and generating the most stable conformation.[20] X-ray diffraction experiments found the distance of the unit cell to be 4.9Å for a representative group of polyphosphazenes, reinforcing this hypothetical portrait of the chain conformation.[10] This distance is consistent with prior results for polymers possessing a cis-trans conformation.

2.3.2 Thermal Properties

The ability to access different morphologies by altering the polyphosphazene substituents is a quality rarely found in many polymer systems. Polyphosphazenes exist over a range from amorphous gums to semicrystalline solids with some of the later materials displaying mesomorphic transformation between the crystallization and melting temperatures.[12] Variations of the side group also greatly influence the glass transition temperature. The transition from the glassy to the rubbery state is contingent upon the size of the substituent and the amount of steric interference.

Since alkyloxy groups are small and non-obstructive, the polymer chain can undergo main chain rotation at low temperatures, usually between -100 to -60°C.[11] The presence of aromatic rings results in increased hindrance of chain motion, causing an elevation in the temperature of the glass transition to between -50 to 0°C. Location and length of the alkyl substituent also influences the glass transition in aryloxyphosphazenes.[12] Meta-substituted phosphazenes have lower glass transition temperatures when compared to para-substituted materials. Increasing the length of the alkyl chain in the para-position also results in the lowering of glass transition temperatures. Amino substituents also have an effect on the chain mobility. Interatomic attractions between the side group and polymer backbone, resulting from increased basicity of the

substituent, limit the chain flexibility and increase the glass transition to above 0°C[21].

The morphology taken on by polyphosphazene materials also depends upon the number of substituents bonded to phosphorus. Mono-substituted polyalkyoxyphosphazenes are semicrystalline, while aryloxy substituted polymers exhibit polymorphic transitions resulting from side chain liquid crystalline formations. These crystalline features relate to the molecular symmetry caused by the presence of a single substituent and the ability of the backbone to reach the preferred cis-trans configuration. The lack of crystallinity in polyphosphazenes results from the presence of two or more substituents. Polyphosphazenes that are di-substituted are amorphous and demonstrate elastomeric capabilities.[3] Table 2 shows the thermal transitions for a variety of polyphosphazene materials.[10]

Table 2. Thermal Transitions of various Polyphosphazenes

Polymer	Tg (°C)	T(1) (°C)	Tm (°C)
$\{(Cl)_2PN\}_n$	-63	---	68
$\{(CH_3O)_2PN\}_n$	-76	---	---
$\{(CF_3CH_2O)_2PN\}_n$	-66	80	240
$\{(C_6H_5O)_2PN\}_n$	5.5	160	390
$\{(p\text{-}CH_3C_6H_4O)_2PN\}_n$	0.3	152	340
$\{(CH_3NH)_2PN\}_n$	14	140	---

2.3.4 Thermal Stability

The thermal stability of polyorganphosphazenes is a physical property that many researchers have disputed. Polydichlorophosphazene displays thermal stability up to 350°C whereupon depolymerization into cyclic oligomers takes place.[22] Allen and others investigated the decomposition for a wide variety of polyorganophosphazenes via thermogravimetric analysis (TGA). The results from these initial experiments demonstrate that a majority of polyphosphazenes possess thermal stability above 300°C. Table 3 shows results from these experiments.[23]

Table 3. Decomposition Temperatures for various Polyphosphazenes

Polymer R group	*% Weight loss*	*Temp(ºC)*	*Temp of 10% loss (ºC)*
Cl	100	550	410
OCH_2CF_3	100	500	410
OC_6H_4Cl(para)	76	600	400
OC_6H_4F(para)	75	500	385
$OC_6H_4C_6H_5$(para)	45	600	470

Allcock and others disputed these preliminary findings.[24] Using polydiphenoxyphosphazene, Allcock performed thermal degradation experiments ranging from 100 to 400°C. The materials, sealed in evacuated heating tubes, were heated to the desired experimental temperatures. The use of intrinsic viscosity, gel permeation chromatography, and mass spectroscopy allowed for investigation of the products from the thermolysis reactions. The results reveal that polydiphenoxyphosphazene undergoes rapid viscosity and molecular weight decreases in the temperature range of 100-200°C. These decreases illustrate the depolymerization. Once depolymerization starts, the formation of a wide variety of cyclic oligomers as well as low to medium molecular weight fragmented polymers occurs. These findings support the possibility that depolymerization is thermodynamically driven resulting from steric interactions in the polymer chain, since these interactions are not present in the cyclic oligomers. The fact that polybistrifluroeythoxy-phosphazene, which has little steric hindrance, is less apt to undergo depolymerization at temperatures below 200°C than polydiphenoxy-phosphazene, reinforces this theory.[25] Because the rate of depolymerization is slow, polydiphenoxyphosphazene is stable at room temperature. However, by increasing the temperature depolymerization becomes favorable. Therefore, hindrance of the depolymerization mechanism would enhance the thermal stability of these polymers.

In his continued investigation into the thermal behavior of polyphosphazenes Allcock[26] observed three particular processes: (1) random chain cleavage of the polymer backbone, (2) depolymerization resulting in the formation of cyclic oligomers, and (3) crosslinking

reactions of the cyclic species to form a network ultrastructure. The samples were heated from 50 to 1000°C in a tube furnace and the products characterized through a combination of ^{31}P NMR spectroscopy, vapor phase osmometry, and mass spectrometry.

Thermogravimetric scan of triflouroethoxyphosphazene illustrates the percent weight loss versus temperature. Trifluorethoxyphosphazene underwent chain cleavage at temperatures below 250°C. The cleavage of the polymer chain arises from low concentrations of imperfections along the polymer chain. These defects result from incomplete substitution of the chlorine atoms during synthesis. At slightly elevated temperatures, the decrease in the molecular weight was complimented by the formation of cyclic oligomers, more specifically, the tetramer $[NP(OCH_2CF_3)_2]_4$ and trimer $[NP(OCH_2CF_3)_2]_3$ species. At temperatures exceeding 300°C, the observation of the depolymerization reaction occurs by plotting the change in the molecular weight and the percentage of oligomers formed against the temperature. This temperature limit is very important because TGA results do not show any appreciable weight loss at or below 300°C, although backbone cleavage and cyclic formation apparently take place below these temperatures. At temperatures above 300°C the cyclic species begins to volatilize and by 450°C the material degrades completely.

Polyaryloxyphosphazenes, phenoxy and p-methylphenoxy, underwent chain cleavage, depolymerization, and subsequent crosslinking upon heating. Molecular weight decreases were observed between the temperatures of 120 - 250°C. The formation of cyclic oligomers was not detected at these temperatures. However, above 250°C for phenoxy and 300°C for methylphenoxy, initiation of oligomer formation takes place. The TGA results demonstrate a significant weight loss occurring at 400°C,

which reflects the volatilization of the oligomers formed during heating. Up to this temperature, these materials' thermal behavior resembles the pyrolytic process of the polyalkylflourophosphazene discussed earlier. At temperatures above 400°C these similarities no longer exist.

Continued heating of the cyclic species yields a viscous solution that eventually hardens at 500°C to form a colorless solid. Further heating produces a darkened mass. The non-volatile solid is the end result of an intermolecular reaction allowing the formation of a network structure. Analysis of the unstable gases given off by the heating of the cyclic compounds reveals the presence of a phenol derivative as the major product. This led the experimenters to theorize that the pyrolytic crosslinking that takes place in aryloxyphosphazenes is a result of reactions that involve the aryloxy substituents themselves. Scheme 3 shows the proposed pathway for this process.[26]

Following depolymerization of the bulk polymer, continued heating of the cyclic oligomers causes heterolytic cleavage of a P-O bond. The result is the formation of a phosphazenium cation and a phenoxide anion. The phosphazenium ion then links itself to the phenyl ring of neighboring cyclic species through electrophillic substitution, creating a chemical crosslink. Additional reactions result in the formation of a network ultra structure. Heating 50/50 mixtures of the $[NP(OC_6H_5)_2]_3$ and $[NP(OC_6D_5)_2]_3$ at various temperatures substantiated these findings. The products, when analyzed by mass spectrometry, showed that exchange between the compounds did occur at temperatures exceeding 400°C. These findings further reinforce the purpose for investigating the degradation behavior of polyphosphazenes. Prior to determining potential high temperature applications of these materials, the controversy

regarding the decomposition and eventual network formation must be resolved.

Scheme 3. The predicted reaction pathway for the formation of a crosslinked product from the depolymerized cyclic species.

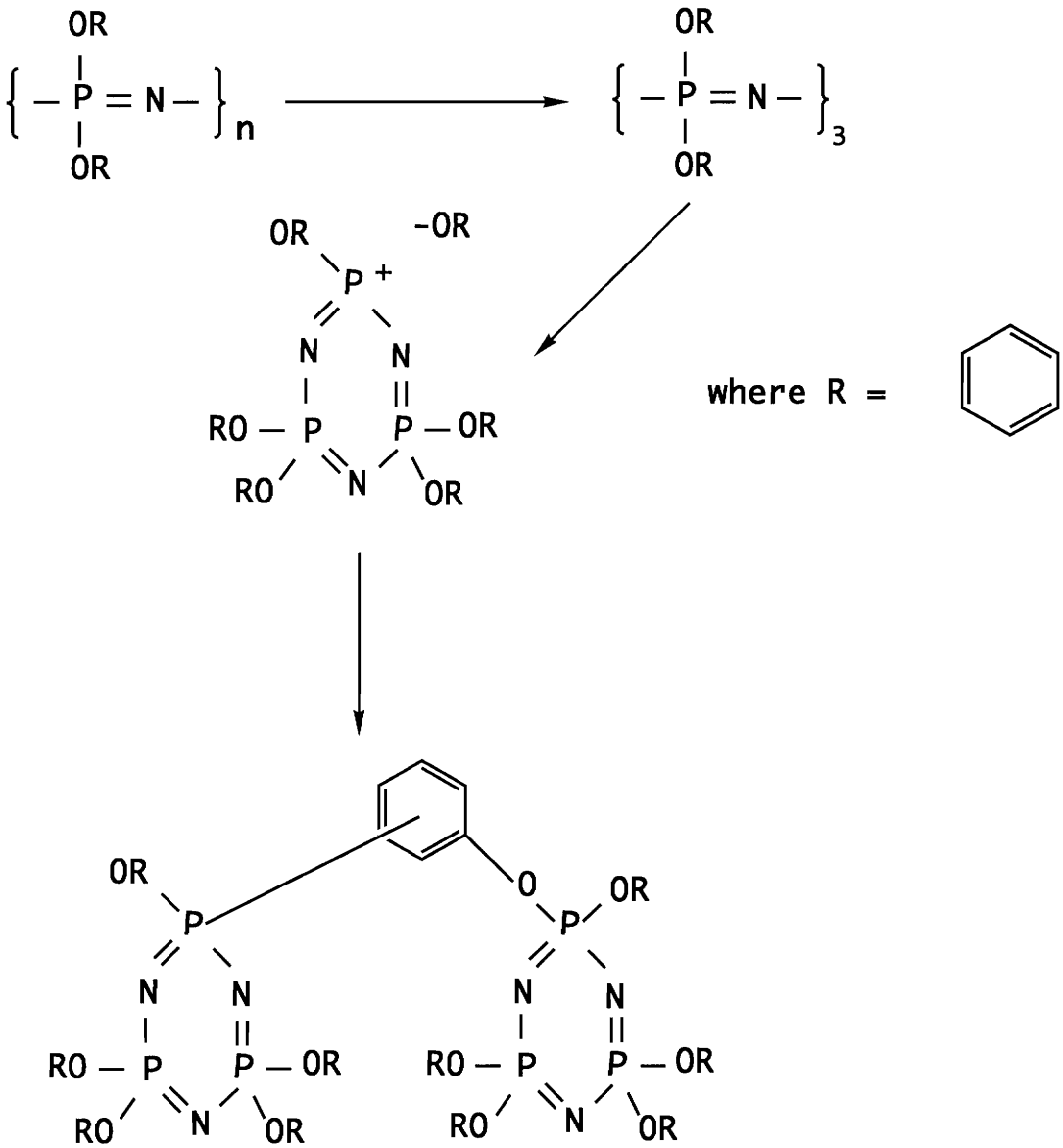

2.3.5 Solution Behavior

Researchers have not extensively investigated the solution behavior of polyorganophosphazenes. The formation of insoluble gelatinous products had hampered the dilute solution characterization of polyphosphazenes. Recent improvements in the synthetic techniques have allowed for dilute solution characterization to become plausible via intrinsic viscosity, membrane osmometry, light scattering, and gel permeation chromatography measurements.

Singler and others performed solubility experiments using a variety of polyphosphazenes but in a limited number of organic solvents. The solvents used possessed solubility parameters ranging from 15.17 to 25.42 $J^{1/2}/cm^{3/2}$.[10] These experiments reveal that semicrystalline polymers are soluble in THF and chloroform at room temperature, as well as in other solvents at moderately elevated temperatures below the mesomorphic transition temperatures. Triflouroethoxyphosphazene is soluble in a number of solvents, but polymers with extended fluorocarbon substituents are only soluble in freon and freon - ether based solvents. Replacement of one or more fluorine atoms with hydrogen atoms in the terminal group of the fluorocarbon chain drastically increased the solubility of the polymer. Polyaminophosphazenes tend to demonstrate polyelectrolytic behavior in dilute acidic media. Alkylamino polyphosphazenes are soluble in acetic

acid alone, whereas phenylamine substituents increase solubility of these materials.

Allen, Lewis, and Todd[13] investigated the dilute solution properties through intrinsic viscosity, gel permeation chromatography, and light scattering measurements reported for a selected group of polyphosphazenes. The researchers reported inconsistent relationships between [η] and weight average molecular weights (Mw). These results, combined with large polydispersity values obtained from GPC and osmometry measurements led them to conclude that polyphosphazenes are highly branched structures. Furthermore, the scientists were unable to measure the radius of gyration through light scattering measurements providing additional evidence that a highly branched structure exists.

Using polyflouroalkoxyphosphazenes Hagnauer and Schneider[27] conducted a similar solution study that resulted in conflicting observations. The intrinsic viscosity and osmometry experiments displayed reproducible results that are consistent with the existence of a linear chain. Light scattering measurements were conducted and the calculated z - average radius of gyration ($<S^2>_z$) was plotted versus Mw. The ratio of $<S^2>_z/M_W$ exhibited consistent values, especially among high molecular weights. The researchers concluded that little chain branching is present because at the higher molecular weights the ratio of $<S^2>_z/M_W$ would become sensitive to side chain branching. Gel permeation chromatography studies again revealed extremely large polydispersity values, which are usually associated with chain branching. Complications during the substitution reactions could possibly explain these unusually large numbers. Improper control of the reaction variables during polymerization could result in difficulties that would affect the formation of

uniform products. Hagnauer and Schneider hypothesized that critical evaluation of narrow molecular weight fractions through GPC would reveal the presence of branching, but had not made this evaluation at the time of their paper.

Continuing the study of polyaryloxyphosphazenes Singler and others[12] performed dilute solution characterization through light scattering, intrinsic viscosity, and membrane osmometry measurements. The results from these experiments led the authors to conclusions parallel to Hagnauer and Scheinder. They found the polymers to have relatively linear chains with small amounts of side chain branching. The authors suggest that the conflicting results between their experiments and Allen's work may have come from incomplete substitution of Allen's materials. Therefore decomposition would occur more easily during the experiments leading to incorrect conclusions.

2.3.6 Mechanical Properties

Early research on the mechanical properties of polyphosphazenes centered primarily around the effects of sample preparation of the materials. Preliminary studies compared the physical variations between solution cast and compression molded films of polyorganophosphazenes.[28] Formation of the solution cast films occurred through the evaporation of THF solutions. These films demonstrated elastomeric

properties and were able to support a load. Compression molding of the polymeric films took place above their respective T(1) transitions. This type of sample preparation yielded brittle materials that would fracture upon the application of minimal force. The morphological differences inherently arise from the variations in sample preparation.

As interest in the mechanical properties of polyphosphazenes grew, Connelly and Gillham investigated their temperature dependencce via torsional braid analysis for a series of polyflouroalkoxyphosphazene homopolymers, copolymers, and blended samples.[29] The polymers were tested over a temperature range of -180 to 250°C and all the samples displayed apparent thermal stability above the final temperature. The loss tangent spectra for the homopolymers revealed glass, crystal-crystal, and melting transitions. The tan delta spectra also revealed secondary glassy - state transitions associated with side chain molecular motions. Variations in these glassy - state transitions when comparing different materials illustrate the substituential dependence of these chain motions. The copolymers exhibited slightly depressed glass transitions with high temperature shoulders. The deconvolution of the single peak revealed a double relaxation occurring leading the authors to believe that the copolymers exist as two phase systems, each dispersion associated with the glass transitions of its respective homopolymer. These materials did not display any crystallization or melting transitions. Finding that the polyphosphazene blends displayed multiple first order transitions, corresponding to the homopolymers that compose the polymer, the authors concluded that the blends also exist as two phase systems. Further investigation of the glassy state secondary transitions and the

influence of substituent size on these transitions were cited as future work by the researchers.

Allen and others[13] conducted a subsequent investigation of the mechanical properties of three representative polyphosphazenes. They used torsion pendulum, vibrating reed and dielectric analyzer to perform their dynamic mechanical experiments. The loss tangent spectra for all of the materials displayed prominent primary transitions in the appropriate temperature range when compared to DSC results. They found the activation energy for the primary transitions of all three materials by plotting the logarithm of the frequency against the inverse of the absolute temperature and evaluating the slope. Table 4 shows the calculated activation energies.[13] These values are larger than one would expect for these materials but the authors made no statements regarding this fact.

Table 4 . Activation Energies for the Glass Transitions determined through Dynamic Mechanical Measurements

Substituent	Activation Energy ΔH (kJ/mol)
Triflouroethoxy	196.7
p-Chlorophenoxy	426.7
p-Phenylphenoxy	340.9

3.0 Solubility Parameter

The solubility parameter acts as a guide for predicting solvent - polymer interactions.[30] This property directly relates to the cohesive energy and cohesive energy density. Hildebrand and others introduced these variables while the exploration of solubility continued. Hildebrand[31] stated that the solubility of a solute in a number of solvents is contingent upon the internal pressure of the solvents. The idea of cohesive energy (E_{coh}) was introduced and defined as the change in the internal energy per mole (ΔU) with regard to the london dipersive forces. Scatchard[32] added to this theory with the principle of cohesive energy density (e_{coh}). This quantity is defined as the cohesive energy per unit volume. Hildebrand[33] continued his investigation of solubility characteristics by proposing that the square root of the cohesive energy density is equal to the solubility parameter (δ). This new quantity provided a means for comparing the behavior of a solute in different solvents. Table 5 illustrates the relationship between all of these variables.

Table 5. Solubility Relationships

$E_{coh} = \Delta U$ $e_{coh} = E_{coh} / V_m$ $\delta = (e_{coh})^{1/2}$

3.1 Estimation of δ

The efforts of Hildebrand and Scatchard demonstrated that the solubility of a solute is mainly a factor of its chemical structure. Equation (1) illustrates that cohesive energy may be calculated by an evaluation of a material's heat of vaporization. However, polymers do not undergo vaporization. Thus, determination of the cohesive energy and related variables occurs by performing comparative swelling or dissolution experiments.

$$E_{coh} = \Delta U_{vap} = \Delta H_{vap} - p\Delta V = \Delta H_{vap} - RT \qquad (1)$$ [33]

Dunkel[34] theorized cohesive energy to be an additive property based upon the chemical structure of a material. This research has since been adapted to polymeric materials. Many researchers have constructed group

contribution tables that approximate the influence of structural components over the cohesive energy and molar volume.

Hayes[35] and Di Benedetto[36] independently developed the first group contribution tables based upon polymer repeat units. Their methods provided fair estimations for the cohesive energy but an inadequate number of structural components were tabulated limiting the applicability. Rheineck and Lin[37] developed a more extensive list of constituents. However, the necessity of numerous corrective measures rendered this method ineffective. Van Krevelen and Hoftyzer[38] attempted to correct these shortcomings by developing more precise group contribution values. Nevertheless, limitations arose from the lack of structural components listed in the table. Finally, Fedors[39]developed a group contribution table that provided less accurate estimations for the cohesive energy than Van Krevelen and Hoftyzer, but more importantly, it allows the cohesive energy to be calculated for a myriad of polymer structures.

3.2 Experimental Determination of the δ

As interest in polymer - solvent interactions grew, Hansen[40] proposed that additional intermolecular forces influence the solubility parameter. Originally, Hildebrand's solubility theories considered london dispersive forces as the only factor affecting polymer - solvent behavior.

Hansen developed a three - dimensional solubility parameter based upon three contributing factors that comprise the cohesive energy. These forces are the polar δ_p, hydrogen bonding δ_h, and london dispersive δ_d components. Equation 2 illustrates the relationship between the variables and the solubility parameter.

$$\delta^2 = \delta_p^2 + \delta_h^2 + \delta_d^2 \qquad (2)$$

By devising an arbitrary rating scale based upon a material's response in various solvents, the solubility parameter can be established. A three-dimensional representation of the solubility parameter components, as a function of the rating system, displays a spherical region of interaction. This interactive sphere encompasses the solvents that imposed the greatest amount of interactions. Defining the center of this spherical region are the components that makeup the solubility parameter of the unknown material. Complications arise during the application of this technique for lack of computer routines that enable three -dimensional manipulation of the experimental data.

Development of a two -dimensional method representation of the contributing forces by Bagely and others[41] successfully corrects this obstacle. The influential forces were separated into two categories, (1) physical and (2) chemical contributions. The london and polar forces categorize as physical elements while the hydrogen bonding effect classifies as a chemical contribution. Equation 3 demonstrates a new term, δ_v, developed to signifying the physical contributions and it's

relationship with the dispersive and polar components. The solubility parameter is then determined thusly as described for the three -

$$\delta_v = (\delta_d^2 + \delta_p^2)^{1/2} \qquad (3)$$

dimensional model except, the region of interaction is circular as opposed to spherical. The components of the solubility parameter are recognized as the center of this circular region and through substitution the solubility parameter of the polymer may be determined.

4.0 Mechanical Properties

Dynamic mechanical properties gauge the response of a material as it undergoes cyclic deformation. Measurements of this kind are important to polymer characterization because the determination of various properties as a function of temperature and frequency are elementary. Measurement of mechanical properties proved to be a useful tool in linking performance to chemical structure in polymers while allowing for the investigation of glass transitions, relaxation phenomena, and morphological transitions.[42]

The dynamic modulus indicates the inherent stiffness of the polymer and ranges from 10^6 to 10^{12} dynes/cm^2 depending upon the polymer structure, experimental frequency, and temperature. Other properties measured from dynamic mechanical experimentation include the loss modulus and loss tangent. Both quantities are sensitive to molecular motions in the polymer chain. Interpretation of these molecular motions lends practical importance in comprehending the temperature and frequency dependence of rotational behavior in polymer chains.[43]

4.1 Theory

These dynamic mechanical experiments are performed by placing periodic forces on a material and monitoring its response to these forces. Several vibrational parameters are key to analyzing mechanical properties such as: stress, strain, amplitude, frequency, and type of oscillation. Depending upon the amplitude of the stress, a linear or nonlinear response will result. To achieve the desired linear response the stress amplitude must be sufficiently small enabling the strain to respond sinusoiudally with time. The amplitude of the strain must be proportional to the stress. In linear viscoelastic behavior, the strain is out of phase with the stress, which is related to molecular motions in the material. These molecular motions are directly related to the energy dissipative relaxation processes in polymer chains.[44]

The equations for the stress, σ, and strain, ε, in dynamic testing are shown below,

$$\sigma = \sigma_0 \sin(\omega t + \delta) \qquad (1)$$

$$\varepsilon = \varepsilon_0 \sin \omega t \qquad (2)$$

in which ω is the angular frequency and δ is the phase angle. Equation (3) depicts an expanded version of equation (1) illustrating how the stress is made up of two components. The first term is referred to as the "in

$$\sigma = \sigma_0 \sin\omega t \cos\delta + \sigma_0 \cos\omega t \sin\delta \qquad (3)$$

phase element", $\sigma_0 \cos\delta$, and the latter as the "out of phase component", $\sigma_0 \sin\delta$. Equation (4) depicts the modulus as having two components after division of the stress by the strain. Two new varables appearing in

$$\sigma = \varepsilon_0 E' \sin\omega t + \varepsilon_0 E'' \cos\omega t \qquad (4)$$

$$E' = \{\sigma_0/\varepsilon_0\}\cos\delta \text{ and } E'' = \{\sigma_0/\varepsilon_0\}\sin\delta \qquad (5)$$

equation (4), E' and E'', are associated with the real and imaginary components of the modulus, respectively. The real component or storage modulus, is associated with the reserve of potential energy and its release upon deformation. The imaginary component or loss modulus is comparable to the dissipation of heat as the material undergoes deformation. The ratio of the loss to storage modulus is the loss tangent

$$\tan\delta = E''/E' \qquad (6)$$

or tan δ. Tan δ is linked to chain mobility and is a ratio of the energy dissipated per cycle to the maximum energy stored during a cycle. These values are commonly related to the internal friction and damping potential of a material.[42]

4.2 Relaxations

One of the most appealing aspects of dynamic mechanical experimentation is the wide range of conditions that may be simulated and tested. The results from a typical dynamic mechanical experiment as a function of temperature are shown below in Figure 3.

Figure 3. Typical dynamic mechanical spectra.

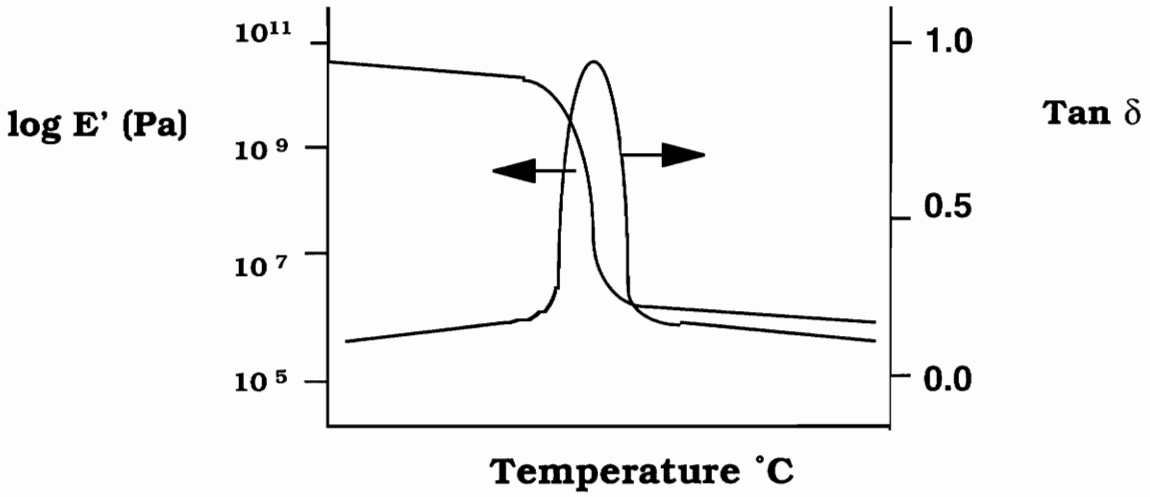

The storage modulus displays a substantial decrease in the stiffness from 10^{11} to 10^{6} dynes/cm^2. This decrease is associated with the transition from the glassy to rubbery state. The tan δ curve shows a maximum height analogous to the modulus inflection point. This

dispersion, is commonly referred to as the primary, or α transition, and represents the glass transition temperature occurring in the amorphous regions of the polymeric material.[45]

Upon reaching the glass transition, an increased amount of vibrational damping abilities become present resulting from the initiation of micro-Brownian motion in the polymer chain. Some chain segments are free to move, while others are still frozen in their orientation. These frozen segments have the ability to store more potential energy than the free segments. As these restrained portions become unfrozen their excess energy is released as heat. The factors that influence the glass transition temperature also affect the α transition, e.g., chain flexibility, substituents' rigidity, and molecular polarity. The amplitude of the primary transition varies depending upon the morphology of the material. Amorphous polymers contain unrestrained chains that possess the freedom to move during the application of thermal energy. This yields large tan δ values. Whereas reduced tan δ values occur when semicrystalline domains hinder the molecular movement of the amorphous chains.[43]

At temperatures below the glass transition, secondary transitions occur. These glassy - state transitions are designated as β , γ, and such, in order of declining temperature. The association of these relaxations with small scale molecular motions such as, side chain and end group rotation, defects in the crystalline lattice, and phase separation consume a majority of the literature on this subject.[43]

Dispersions are also evident at temperatures above the α relaxation. Those occurring between the glass transition and melting temperatures result from molecular motions in the crystalline regions of a material. The molecular motions associated with these relaxations come about from chain folding and

expansion of the crystal lattice. The symbol α_c or α' represents this relaxations.[42] In amorphous polymers these dispersions result from melting phenomena[46] or molecular motions of low molecular weight fractions of polymers possessing broad molecular weight distributions.[47]

5.0 Thermal Analysis

The definition of thermal analysis embodies all techniques that encompass the measurement of a physical property of a substance and/or its reaction products as a function of temperature.[48] Even though this definition enlists a wide variety of methods, a majority of the experiments reported in the literature involved the application of only a few instruments. The thermogravimetric analyzer (TGA) monitors mass loss or gain, while a differential scanning calorimeter (DSC) measures the change in specific heat capacity, and finally dynamic mechanical (DMTA) and dielectric (DETA) thermal analyzers yield the storage and loss moduli. The use of these techniques in conjunction with evolved gas instruments and various forms of spectrometers is common place. This research focuses on thermogravimetric analysis and its possible applications.

5.1 Thermogravimetric Analysis

By definition, thermogravimetry is the measure of any reaction involving mass change as a function of temperature. The conventional use of a TGA involves the investigation of thermal degradation in vacuum,

inert, or active atmospheres. The use of this medium to predict service lifetime and thermal breakdown limitations is widely accepted. Recent, other uses for the TGA include: measurement of the glass transition temperature[48], evolution of volatile gases during pyrolysis, and determination of degradative kinetics.

The determination of kinetic degradation parameters from thermogravimetric data recently became a widely accepted method since its introduction by Freidman[49]. The kinetic treatment begins with the manipulation of the Arrhenius equation (1) where A is the pre-exponential factor, E is the activation energy, and R is the universal gas constant.

$$k(T) = A \exp(-E/RT) \qquad (1)$$

Substitution for the fractional degradation of the polymer results in equation (2).

$$d\alpha/dt = f(\alpha)A \exp(-E/RT) \qquad (2)$$

Equation (3) shows a relationship between the activation energy, ΔE, and the degree of conversion, α_i, where $(d\alpha/dt)_i$ and T_i are the rate of conversion and temperature, at which α_i is reached.

$$\ln(d\alpha/dt)i = \ln Af(\alpha_i) - (\Delta E/R)(1/T_i) \qquad (3)$$

Using equation (3) the plot of $\ln(d\alpha/dt)i$ vs $(1/T_i)$, results in a slope proportional to the activation energy. Performing this procedure at various degrees of conversion determines the consistency of the activation energy.

Ozawa [50] and Flynn[51], independently, improved this method by using constant heating rate experiments and determining the activation energies for the degradative process at particular degrees of conversion. Flynn suggested that by comparing the same degree of conversion for several experiments of different heating rates, determination of the kinetic parameters was possible. The Arrhenius equation was the basis for Flynn's isoconversional method and substitution for the fractional conversion was the same as shown earlier (4).

$$d\alpha/dt = f(\alpha)k(T) \qquad (4)$$

Substituting a constant heating rate, $\beta = dT/dt$, into equation (4) yields the conversion as a function of temperature instead of time. Integration of equation (5) results in an equation for the fractional conversion shown in equation (6). The use of Doyle's approximation to equation (7) becomes necessary since the integral does not converge. Rearrangement of equation (8) illustrates that the activation energy is proportional to the slope of ln β versus 1/T (K). All of these equations are shown below (5-8).

$$d\alpha/dT = \beta^{-1}f(\alpha)k(T) \qquad (5)$$

$$F(\alpha) = \int (d\alpha/f(\alpha)) = \beta^{-1}\int k(T)dT \qquad (6)$$

$$F(\alpha) = A\beta^{-1}\int \exp(-E/RT)\, dT \qquad (7)$$

$$\ln F(\alpha) = \ln (AE/R) - \ln \beta - 5.3305 - 1.052(E/RT) \qquad (8)$$

The series of plots obtained from this method illustrate whether the temperature dependence follows the Arrhenius equation. Parallel slopes for different degrees of conversion result in equal activation energies and an

Arrhenius dependence. Inconsistencies in these values demonstrate that the simple kinetic equations used to develop this method inadequately explain the degradative mechanisms of the material.[52] The most important aspect of the isoconversional method is that it allows for the calculation of the activation energy without having to give consideration to $f(\alpha)$ that proves to be an elusive measurable quantity.

6.0 Experimental

6.1 Materials

The polyphenoxy - ethylphenoxyphosphazene was provided by CSA Engineering of Palo Alto, CA and was used in all experiments. This di-substituted phosphazene possessed a non-transparent white appearance and exhibited elastomeric properties prior to experimentation. Information was not provided by the manufacturer regarding the synthetic formation, possible molecular weight distributions or topology of the material. Figure 4 is a representation of the repeat unit for polyphenoxy-ethylphenoxy-phosphazene.

Figure 4. Repeat unit of polyphenoxy-ethylphenoxyphosphazene

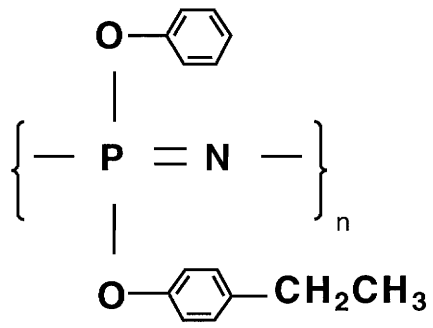

6.2 Solution Investigation

By determining the invulnerability a material possesses to specific solvents, one can qualitatively predict sealant performance. The examination of the solubility parameter of polyphenoxy-ethylphenoxy-phosphazene provides insight regarding the solvent resistive capabilities of this material. Comparative dissolution or swelling experiments were performed in various solvents and an experimental solubility parameter was determined. The solubility experiments were performed by placing a small amount of sample in a variety of organic solvents having solubility parameters ranging from 14.8 to 48 $J^{1/2}/cm^{3/2}$ [30]. Consistent amounts of material were placed in each solvent and all experiments were performed at room temperature. The weight gain of the material was monitored in the various solvents and the results were plotted against the solubility parameters of the solvents to determine an experimental solubility parameter. Upon completion of the solvent ingression experiments each sample was dried and weighed to determine the sol - fraction. Weight gain measurements were performed using a Metler digital balance AE 2000. Comparison of the experimentally determined solubility parameter to an estimated value from Fedors'[39] group contribution tables determined the applicability of this additive procedure to phosphazene structures.

6.2 Thermal Analysis

The induction of thermogravimetric analysis established the thermal stability relationship to polyphenoxy-ethylphenoxyphosphazene while also setting an upper temperature limit of application. A properly calibrated Perkin-Elmer TGA 7 analyzed these temperature dependent functions with a calcium oxalate standard and achieved acceptable results based upon manufacters specifications. Two separate sets of experiments were conducted using oxygen and nitrogen, independently as purge gases, to determine the effect of atmosphere on the degradation process of polyphenoxy-ethylphenoxyphosphazene. The samples were heated from room temperature to 800°C with heating rates ranging from 5°C/min to 25°C/min in accordance with Flynn's isoconversional methodology. The sample sizes ranged from 18-21 mg.

6.4 Dynamic Mechanical Evaluation

While setting a lower temperature limit of application, the vibrational damping ability of polyphenoxy-ethylphenoxyphosphazene, was examined

via dynamic mechanical experiments. A Perkin Elmer DMA 7 in the three point bend mode was used to perform the dynamic mechanical analysis. This method was selected based upon the sample size and the elastomeric characteristics the specimen exhibited on preliminary inspection. Mounting of the samples transpired using a 15mm bending platform. The cyclic force was distributed using a 3mm sphere probe tip. All experiments utilized the same sample sizes: width 15mm, depth 5mm, and height 3.2mm. The tests were performed using the temperature scan program in which the temperature was ramped from -100 to 100°C at 1°C/min with the frequency, dynamic and static stresses remaining constant. Experimental frequencies ranged from 1 to 50 Hz.

7.0 Results and Discussion

7.1 Solution Properties

7.1.1 Estimation of δ

The solubility parameter for a given polymeric material can be estimated using group contribution theories and tables. Fedors' estimated the group contributions for the energy of cohesion (Δe_i) and molar volume (Δv_i) for a broad number of structural components. A summation of these values, according to a material's repeat unit, enables one to estimate the cohesive energy (ΔE_V) and molar volume (V). The ratio of these values is equal to the solubility parameter as shown in table 6.

Table 6. Additive Equations for the Calculating the Solubility Parameter

$$\Delta E_{coh} = \Sigma_i \Delta e_i$$
$$V = \Sigma_i \Delta v_i$$
$$\delta = (\Delta E_{coh}/V)^{1/2}$$

The repeat unit of polyphenoxy-ethylphenoxy-phosphazene was the basis for construction of Table 7. It shows the approximate values for the contributions of the energy of cohesion and molar volumes for each structural component. Summation of the contributions results in the cohesive energy and molar volume, as well as the estimated solubility parameter.

Table 7. Calculation of Solubility Parameter using Fedor's Group Contribution Tables

structural component	Δe_{vi}(J/mole)	Δv_i(cm^3/mole)
P	9414	-1.0
-N=	11715.2	5.0
2(-O-)	2(3347.2)	2(3.8)
Phenyl	31923.9	71.4
p-Phenyl	31923.9	52.4
CH_2	4937.1	16.1
CH_3	4707	33.5
	$\Sigma\Delta e_{vi}$ = 101315.5	Σvi = 185.0

$$\delta = (101315.5/185.0)^{1/2} = 23.4 J^{1/2}/cm^{3/2}$$

The estimated solubility parameter for polyphenoxy-ethylphenoxy-phosphazene was 23.4 $J^{1/2}/cm^{3/2}$ using Fedors' contribution tables. Comparison of an experimentally determined solubility parameter to the approximated value will determine whether Fedors' contribution tables are applicable to phosphazene systems.

7.1.2 Solubility Study

The selection of the solvents for solvent ingression experiments was based on solubility parameters, allowing the investigation of a wide range of solvent- polymer interactions. Table 8 shows a list of solvents used and their respective solubility parameters.[30] By monitoring the response of a material in various solvents, determination of the unknown polymer's solubility parameter is possible. A plot of the percent weight gain versus the solubility parameters of the solvents passes through a maximum associated with increased polymer - solvent interactions and the solubility

Table 8. Solvents used in the Solubility Study and their Solubility Parameters and the components thereof. All the solubility parameters have units of $J^{1/2}/cm^{3/2}$

Solvent	δ	δ_h	δ_d	δ_p
methanol	29.5	22.3	5.2	12.3
water	48.0	34.2	13.3	31.3
ethanol	26.5	19.5	15.8	8.8
acetonitrile	24.3	6.1	18.8	18.0
chloroform	19.0	5.7	17.9	3.1
CH_2Cl_2	19.9	6.1	16.8	6.4
2-propanol	23.6	16.4	15.8	6.1
p-xylene	17.9	1.0	16.9	1.0
1,2-propanediol	30.3	23.3	16.9	9.4
toluene	18.2	2.0	17.7	1.4
DMF	24.9	11.3	17.4	13.7
hexane	14.8	0.0	14.8	0.0
methyl pyrrolidone	22.9	7.2	17.9	12.3
acetone	20.2	7.0	15.5	10.4

parameter of the unknown material.

The polyaryloxyphosphazene material proved to be insoluble in all solvents tested. The polymer displayed significant weight gain in some solvents while minimal gain in others. Table 9 shows the weight gain for each of the solvents. The material reached equilibrium weight in less than 40 hours. A plot of the percent weight gain versus time shows exponential

*Table 9. Weight gain for the various solvents. Wo is the original weight in milligrams, W is the weight gain in mg after 96 hrs and the percent weight gain was calculated by the following equation {{W-Wo}/Wo}*100*

Solvent	Wo	W @ 96 hours	% wt. gain
methanol	64.64	66.72	3.22
water	64.2	65.90	1.98
ethanol	63.80	67.21	5.23
acetonitrile	65.72	72.00	9.56
chloroform	64.83	297.54	358.95
CH_2Cl_2	70.22	265.10	277.53
2-propanol	64.18	68.54	6.79
p-xylene	70.42	216.53	207.49
1,2-propanediol	61.34	65.78	7.24
toluene	70.58	217.36	207.96
DMF	61.72	140.00	126.83
hexane	60.69	77.62	27.90
Me-pyrrolidone	66.48	77.21	16.14
acetone	70.91	110.16	55.35

growth in the weight with respect to time. When the plateau is reached, one can safely assume that an equilibrium has been established. Figure 5 depicts the experimental weight versus time for polyphenoxy-ethyl-phenoxyphosphazene in chloroform.

Figure 5 Percent Weight Gain Versus Time i in chloroform illustrating the equilibrium weight being reached in a short time period.

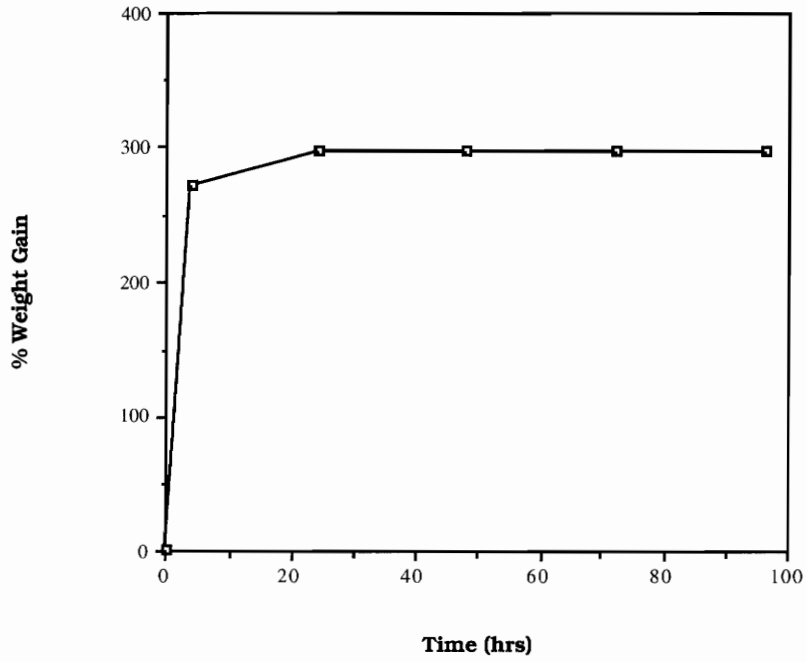

The insolubility of the polymer is representative of a material possessing a crosslinked topology. The crosslinked nature of the polymer combined with the quickly achieved equilibrium weight leads one to conclude that the polyphenoxy-ethylphenoxyphosphazene exists as a lightly crosslinked network.

The solubility parameter is directly related to solvent-polymer interactions. The solvents that induce the greatest amount of swelling are interacting with the polymer to a larger extent than the other solvents. On the basis of solubility parameter determined from Fedors' group contribution tables, the solvents that should interact with polyphenoxy-ethylphenoxyphosphazene are 2-propanol, acetonitrile, and dimethylforamide. This was not the case. The solvents chloroform, methylene chloride, and toluene displayed the greatest weight gain. These solvents possess solubility parameters of approximately 19 $J^{1/2}/cm^{3/2}$. This represents a significant deviation from the estimated solubility characteristics. Figure 6 shows the experimental weight gain as a function of each solvent's solubility parameter. The curve shows a maximum analogous to the experimental solubility parameter which is 19.3 $J^{1/2}/cm^{3/2}$.

Figure 6 Percent Weight Gain versus The Solubility Parameter of the Solvents.

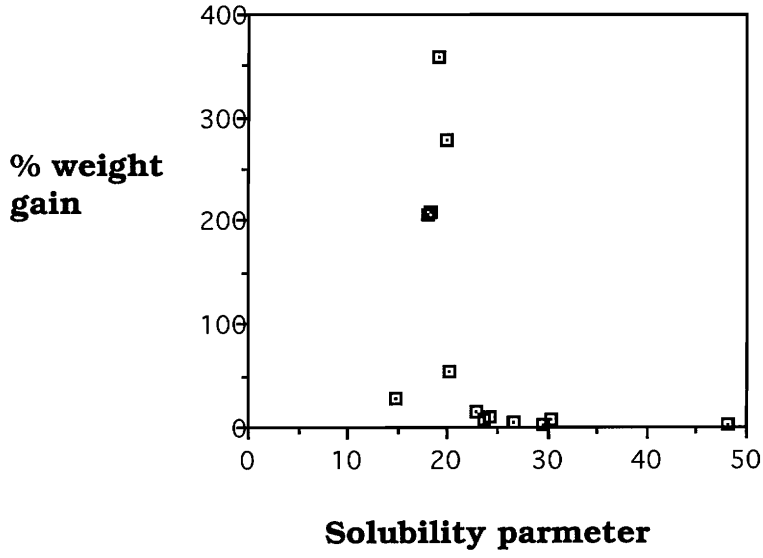

Investigation of the effects that intermolecular forces imposed upon swelling behavior lead to the development of an arbitrary rating scale. The rating scale was based upon the observed weight gain in a given solvent. Weight gains of greater than 150% received a rating of 3, 150% to 50% got a rating of 2, and below 50% received a rating of 1. The solubility parameter of the polyphenoxy-ethylphenoxyphosphazene was established by plotting physical (δ_v) and chemical contributions (δ_h) of the solvents as function of the rating system. This plot is shown in figure 7.

Figure 7 Two - Dimensional representation of the physical and chemical contributions to the solubility parameter.

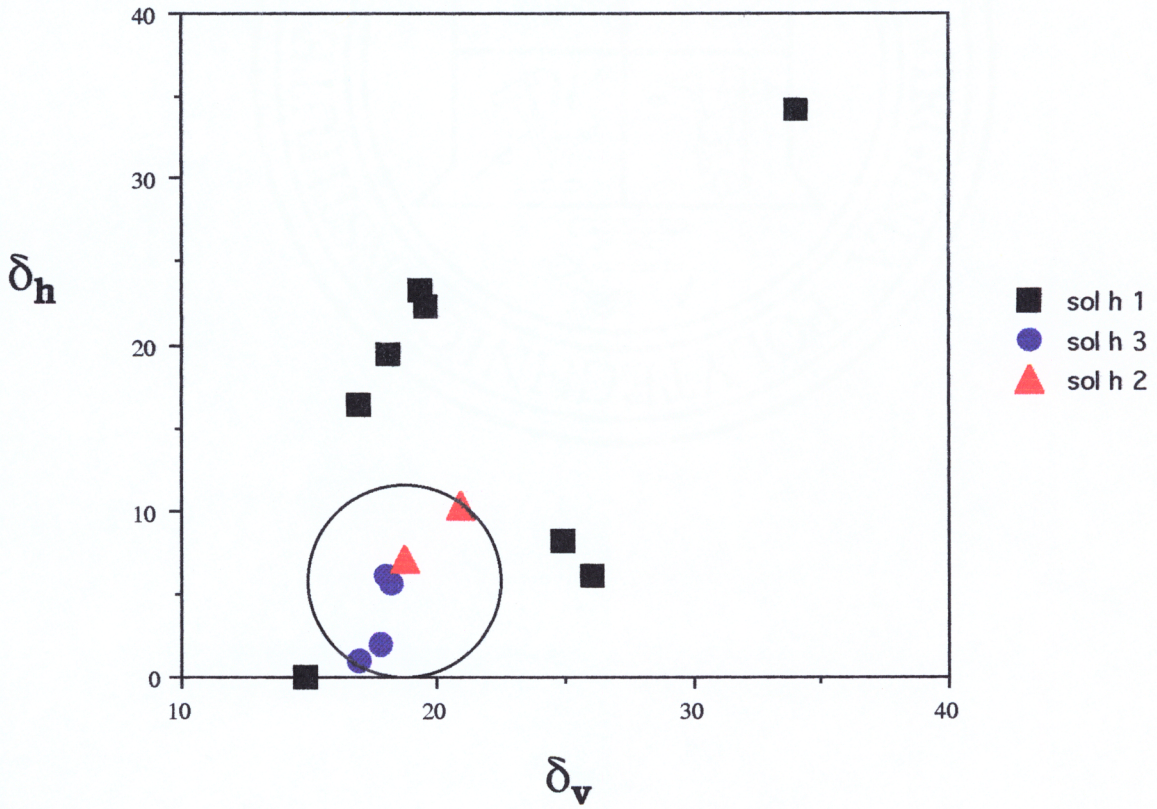

The blue dots represent the greatest amount of polymer - solvent interactions indicative of increased swelling. The red triangles depict intermediate interactions while the black boxes portray minimal interactions. The circular region encompassing the blue and red dots illustrates increased solvent interactions. The center represents the physical and chemical contributions of the solubility parameter of polyphenoxy-ethylphenoxyphosphazene. The coordinates of this interactive sector are (18.5, 5.2) corresponding to the δ_v and δ_h components, respectively. Using these components values and substituting them into the proper equations, the solubility parameter for polyphenoxy-ethylphenoxyphosphazene is 19.2 $J^{1/2}/cm^{3/2}$. This evaluation embodies the key role that intermolecular forces play in the cohesive properties of polymeric materials and reinforcing the applicability of Hansen and Bagley's theories.

Another way of illustrating the influence of intermolecular forces is to construct a graph displaying the components of the solubility parameter for each solvent as a function of the rating system. Figure 8 illustrates any trend that may exist between the individual components of the solubility parameters and the extent of solvent-polymer interactions. The graph shows that increased solvent-polymer interactions occur in solvents when the polar and hydrogen bonding components range from just above 1.0 to 10 $J^{1/2}/cm^{3/2}$. Intermediate solvent-polymer interactions were observed for solvents with slightly higher values for the δ_h and δ_p but below 13 $J^{1/2}/cm^{3/2}$. Some solvents possessed a low δ_p and a high δ_h or vice versa. These solvents did not interact with the polymer. The dispersive components are essentially equal for all of the

solvents and therefore no correlation relating its effect on the solubility is available. However, an observable trend exists between the solvent-polymer interactions and the components of the solubility parameter. Polyphenoxy-ethylphenoxyphosphazene demonstrated increased interactions with solvents in which the polar and hydrogen bonding contributions were minimal.

Figure 8 The components of the solubility parameter versus the rating system illustrating the effects of individual components

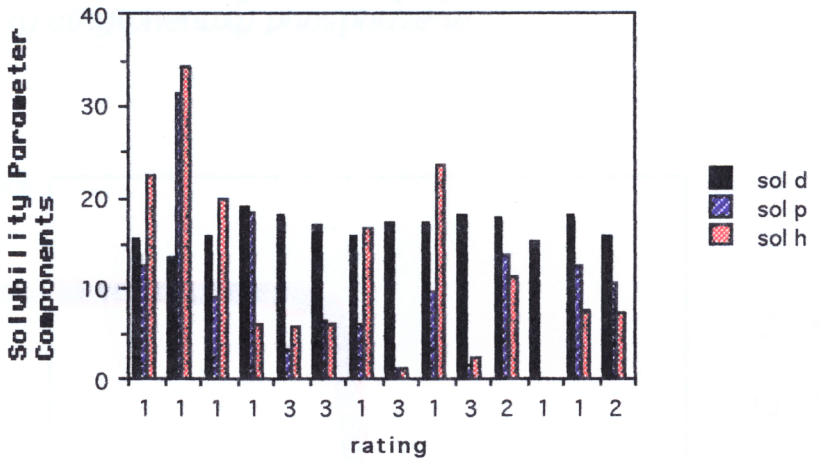

A list of the values obtained from the three methods outlined for determining the solubility parameter are shown below.

Method	δ ($J^{1/2}/cm^{3/2}$)
Fedors' group contribution	23.4
swelling experiment	19.3
component evaluation	19.2

Each method gave different results for the solubility parameter of the material. Fedors' group contribution tables depicts a significantly larger value than the experimental quantities but provides a viable estimation. This discrepancy stems from the attempt to use experimental results based upon low molecular weight compounds to explain polymer behavior. Also the basis for the group contribution theories regarded the dispersive forces as the only influential factor on polymer - solvent interactions. The results shown in this section demonstrate that polar and hydrogen bonding forces exert additional influences on polymer - solvent interactions. Sealant applications are most favorable in highly polar and hydrogen bonding environments that keep polymer-solvent interactions to a minimum.

Upon completion of the solvent ingression experiments each of the samples were dried and comparisons of the final and original weights illustrated the effect of polymer solvent interactions. The solvents that displayed increased interactions with the polymer showed significant weight losses while minimal weight loss was observed in less interacting solvents.

Both experimentally determined solubility parameters presented similar values with less than 5% deviation between the two calculated results. Each technique illustrates the effect intermolecular forces place upon polymer- solvent interactions and either method would be sufficient in characterizing a material.

7.2 Thermal Stability

Thermogravimetric analysis of polyphenoxy-ethylphenoxy-phosphazene shows that the material possesses an apparent thermal stability to temperatures above 400°C in both air and nitrogen atmospheres. Figure 9 compares both of these thermal profiles and shows the effect that atmospheric conditions have upon degradative kinetics.

Figure 9. Thermal degradation profiles in air and nitrogen for poly-phenoxy-ethylphenoxy phosphazene

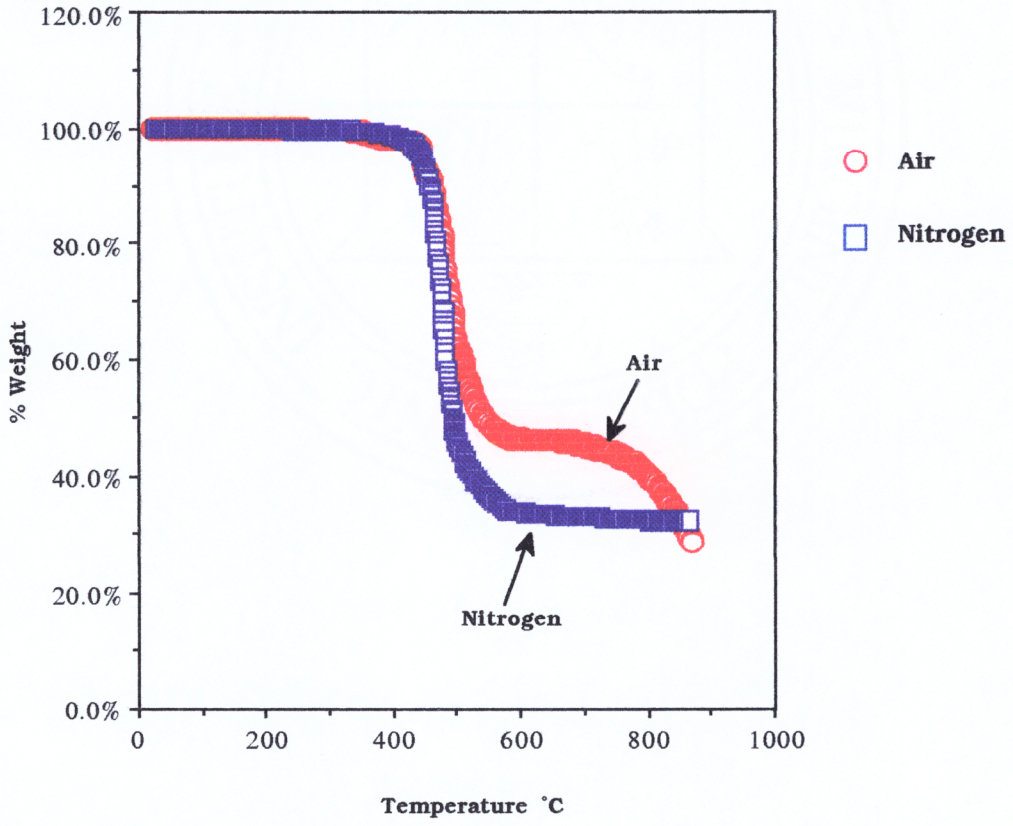

The difference in this degradative behavior results from dissimilar degradation mechanisms. Allcock and others looked extensively at the degradation of polyaryloxyphosphazenes in nitrogen atmospheres and the outcome of these experiments was discussed in section 2.3.2. The scientists concluded that polyaryloxyphosphazene systems do not possess the thermal stability that TGA experiments suggest. These polymeric systems tend to undergo chain cleavage and depolymerization yielding cyclic and oligomeric species. A subsequent crosslinking reaction of the non-volatile cyclic and oligomeric products takes place upon further heating fostering the formation of pyroltic black solid residue.

The thermal profile for phenoxy-ethylphenoxyphosphazene appears similar in all respects to Allcock's research with exception of a shift to slightly higher temperatures during the degradation of the material. This increase equates to the difference in polymer substituents.

The depolymerization of the polymer chain into cyclic oligomers is not evident in either of the thermal profiles. The sharp decrease in the percent weight loss at temperatures exceeding 400°C reflects the volatilization of these cyclic species. At temperatures above 500°C, the decrease in percent weight loss ceases and a pyrolitic black solid forms. This process is evident from the thermal profile in figure 8. The formation of the non-volatile solid results from intermolecular coupling reactions, involving the loss of a phenol based group. This behavior is characteristic only of polyaryloxyphosphazenes. The proposed pathway for the formation of the network relies on the cleavage of P-O bonds to form phosphazenium cations and phenoxide anions. The phosphazenium ion couples with a phenyl ring of a second phosphazene. Formation of a crosslinked material

occurs through additional coupling reactions of this kind. Scheme 3 found in section 2.3.4 illustrates this process.

Thermogravimetric analysis reveals that the thermal profiles in nitrogen and air environments are similar apart from the crosslinking reaction taking place at lesser degrees of conversion in an air environment. In nitrogen, the network formation developed at about 60% conversion while in air, the crosslinking occurred at about 50% conversion. Air provides a harsher degradative environment, allowing the heterolytic cleavage of the P-O linkages to occur at lower temperatures. The network formation results and the remaining volatile species are evolved reflected by the decrease in the percent weight loss at the end of the thermal profile.

Using Flynn's isoconversional method, investigation of the activation energies for the degradative mechanisms of polyphenoxy-ethylphenoxy-phosphazene occurred. These experiments were conducted under identical conditions with the exception of the heating rates. Rearrangement of equation (1) illustrates that the activation energies are proportional to the slope of the ln β vs 1/T(K), at different points of conversion.

$$\ln F(\alpha) = \ln (AE/R) - \ln \beta - 5.3305 - 1.052(E/RT) \quad (1).$$

The isoconversional plot for polyphenoxy-ethylphenoxyphosphazene in nitrogen, found in figure 10, shows that at different points of conversion the slopes of the plots are essentially equal. The invariance in the slopes illustrates that the activation energies are equivalent until 60% conversion

is reached. The homogeneity of the activation energy demonstrates that the degradation of polyaryloxyphosphazene in nitrogen follows the simple Arrhenius kinetic equation. The calculated activation energies are shown in table 10 with a global activation energy found to be

Figure 10. Isoconversional plots for polyphenoxy-ethylphenoxyphosphazene in nitrogen at different points of conversion.

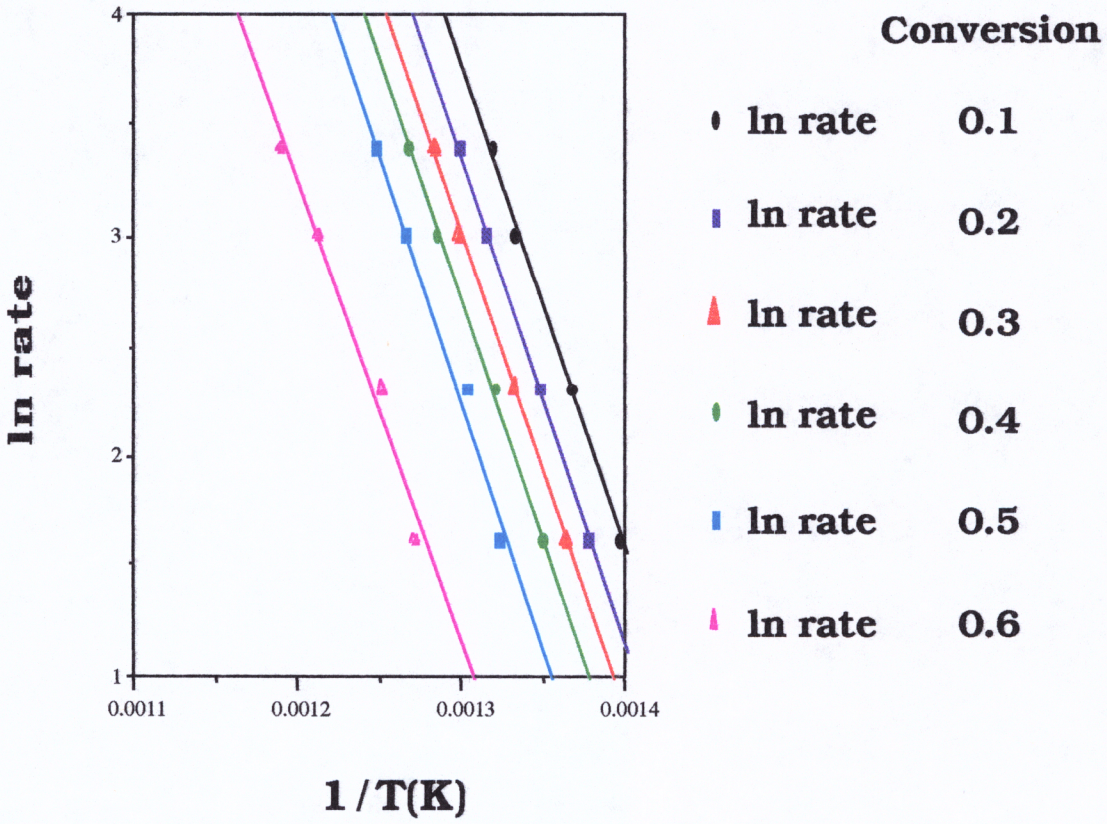

Table 10 . Calculated activation energies in nitrogen.

Conversion	*Actvation energy(kJ/mole)*	
0.1	176.3	
0.2	175.6	
0.3	173.7	global activation energy
0.4	172.2	175.14 kJ/mol
0.5	177.9	
0.6	164.6	

175.2 +/- 2.4 kJ/mol. This global activation energy is associated with the volatilization of the cyclic species that ceases at 60% conversion. At this point of conversion, the crosslinking reaction is beginning to take place altering the reaction kinetics and decreasing the activation energy.

The isoconversional plot for polyphenoxy-ethylphenoxyphosphazene in an air atmosphere, shown in figure 11, does not display the same simple kinetic relationship as was shown in nitrogen. The slopes of these lines are not equal at different points of conversion. This suggests that the Arrhenius equation is inadequate for explaining the complex mechanistic process that is occurring. The activation energies for the volatilization of the cyclic species and network formation are not as distinguishable as in nitrogen. The difference in the activation energies between the two atmospheres can be related to the oxidative abilities of air. Based on the findings by Allcock and the results reported in this paper, the upper

temperature limit for sealant application of polyphenoxy-ethylphenoxy-phosphazene is 200°C in both air and nitrogen environments.

Figure 11 Isoconversional plot for polyphenoxy-ethylphenoxyphosphazene in air at different points of conversion..

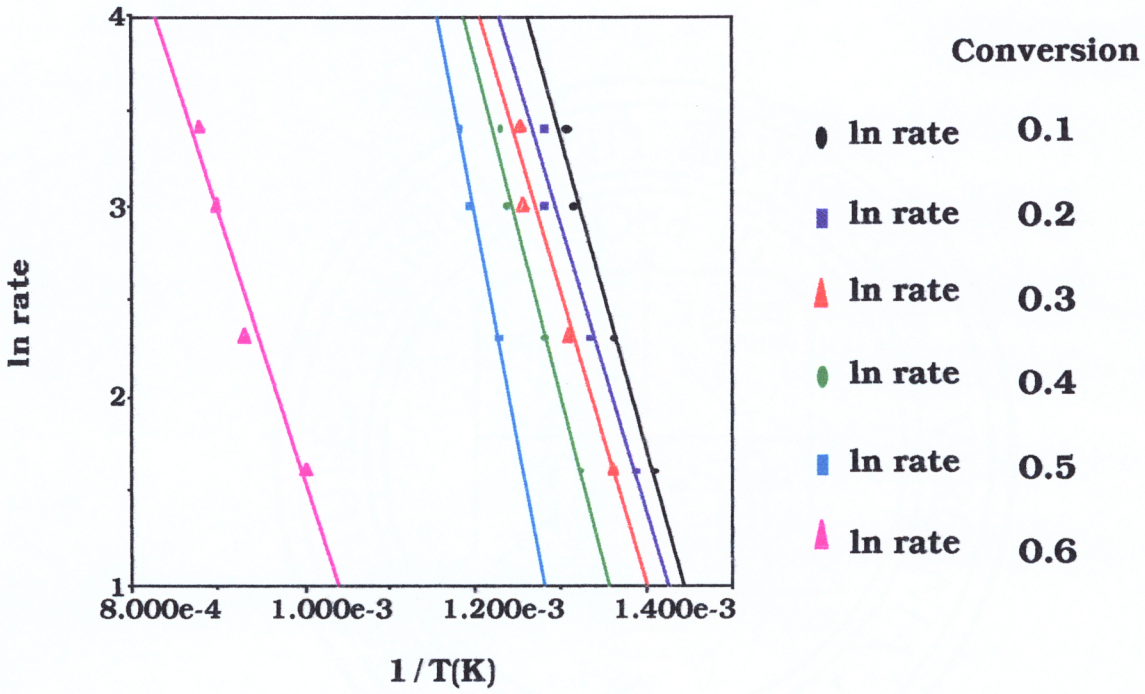

7.3 Dynamic Mechanical Evaluation

Dynamic mechanical experiments using polyphenoxy-ethyl-phenoxyphosphazene permitted the characterization of vibrational damping abilities and established a lower temperature limit of sealant application. Figure 12 shows the storage modulus and tan δ plotted on a double y- axis as a function of temperature. In the glassy state, the material exhibits a storage modulus of slightly less than 10^9 Pa and after passing through the glass transition it reaches a rubbery plateau. The latter behavior is distinctive of crosslinked materials. The transition from the glass to rubbery state begins at -20°C and concludes at 20°C with a storage modulus of the rubbery regions of 10^6 Pa.

The spectrum of tan δ displays a prominent double relaxation ranging from -20°C to 30°C. The first peak is associated with main chain cooperative motion and the glass transition of polyphenoxy-ethylphenoxy-phosphazene. The second dispersion, which occurs at temperatures above the glass transition, offers several possible explanations. The first relates to the aryloxy substituents of the material. This peak could be perceived as a crystalline transition. Experimentation extinguished this theory when a melting transition did not occur at final temperatures of 220°C. Other possibilities are linked to the manufacturer, suggesting potential filler materials or synthesis complications. Conformation of this information was not received. However, the intricacies involved in the synthesis of these materials are numerous and previously discussed in section 2.2.

Figure 12. Dynamic Mechanical Spectra of Polyphenoxy-ethylphenoxyphosphazene log E' and Tan δ Vs temperature

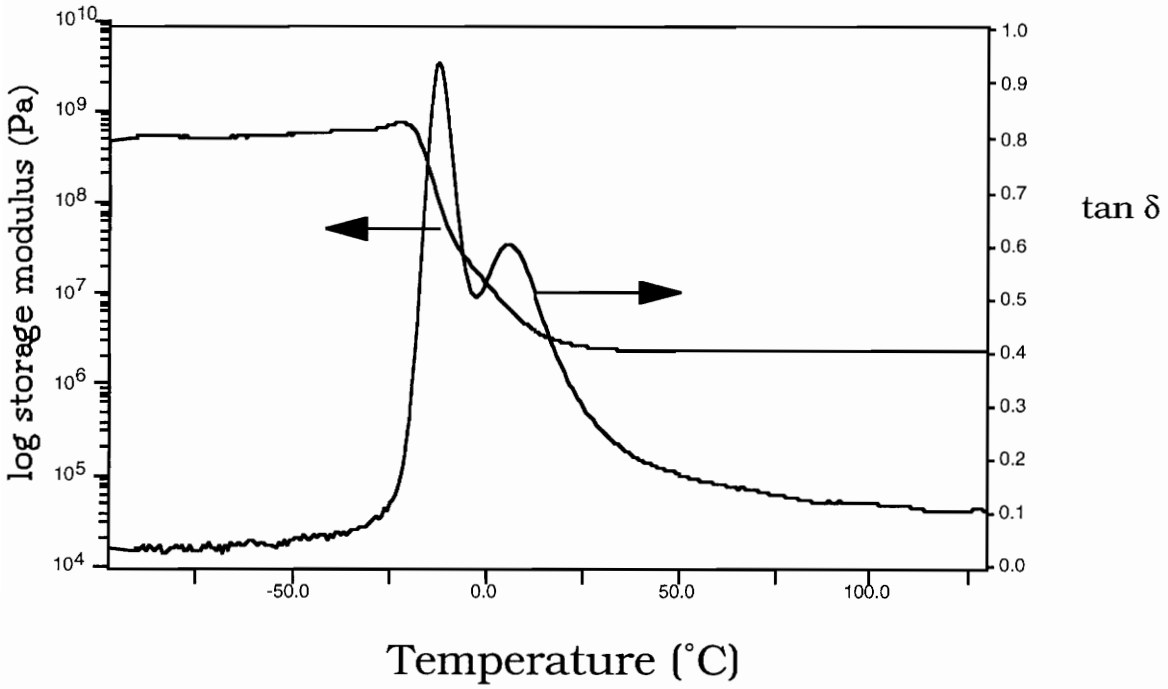

By not accurately controlling the addition of the nucleophilic agents improper substitution causes the formation of a copolymeric material. As mentioned in section 2.3.6, dynamic mechanical analysis of polyphosphazene copolymers displays two prominent relaxations each associated with the glass transition of the homopolymer. If this theory is correct the material must exhibit some phase separation. Scanning electron microscopy was performed on the material and showed evidence of phase separation in the material. Figure 13 displays these micro graphs. The gray areas represent the continuous phase of polyphenoxy-

ethylphenoxyphosphazene. The smaller white domains depict the existence of a second phase. Therefore the second peak results from the presence of a second material which in all likelihood is either diphenoxy or diethylphenoxyphosphazene. The glass transition of diphenoxy-phosphazene is 10°C while diethylphenoxyphosphazene's is 25°C. By process of elimination the second phase might be diphenoxyphosphazene. The glass transition is slightly depressed due to the presence of the polyphenoxy-ethylphenoxyphosphazene. Nuclear magnetic resonance in the P^{31} mode on the solid and swollen state proved to be inconclusive and did not aid in the identification of the second phase. Differential scanning calorimeter experiments revealed a very broad single transition over an identical temperature range as discussed previously. Figure 14 shows these results. The glass transition was taken as the midpoint of the endothermic process and found to be -16°C.

The significance of this second peak is critical to the vibrational damping abilities of this material. The amount of vibrational damping energy a material can dissipate is proportional to the area under the tan δ curve. The presence of the supplemental phase in essence doubles the vibrational damping capabilities of the material and in doing so increases the temperature range at which the sealant applications of this material are possible. The lower temperature limit of application is essentially the point at which the vibrational damping diminishes. Therefore this material is suitable for application to temperatures just below -10°C. Multiple frequency spectra of the copolymer is represented in figure 14. As the frequency increases, both peaks shift to higher temperatures. Increasing the frequency gives the molecular chains less time to relax. Consequently, the shift to higher temperatures occurs. This response

illustrates that vibrational damping properties are not only dependent upon the temperature but also frequency. This frequency dependence

Figure 13 . Scanning Electrographs of Polyphenoxy-ethyl-phenoxyphosphazene. copolymerized with an unknown second phase

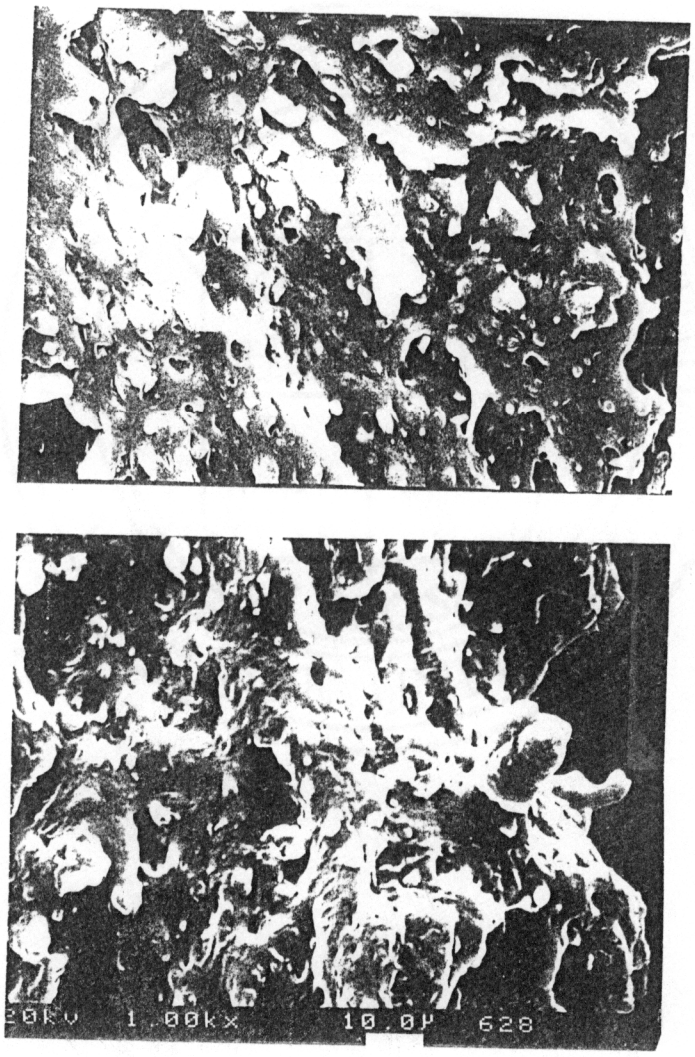

Figure 14. Differential Scanning Caliometer results in Nitrogen

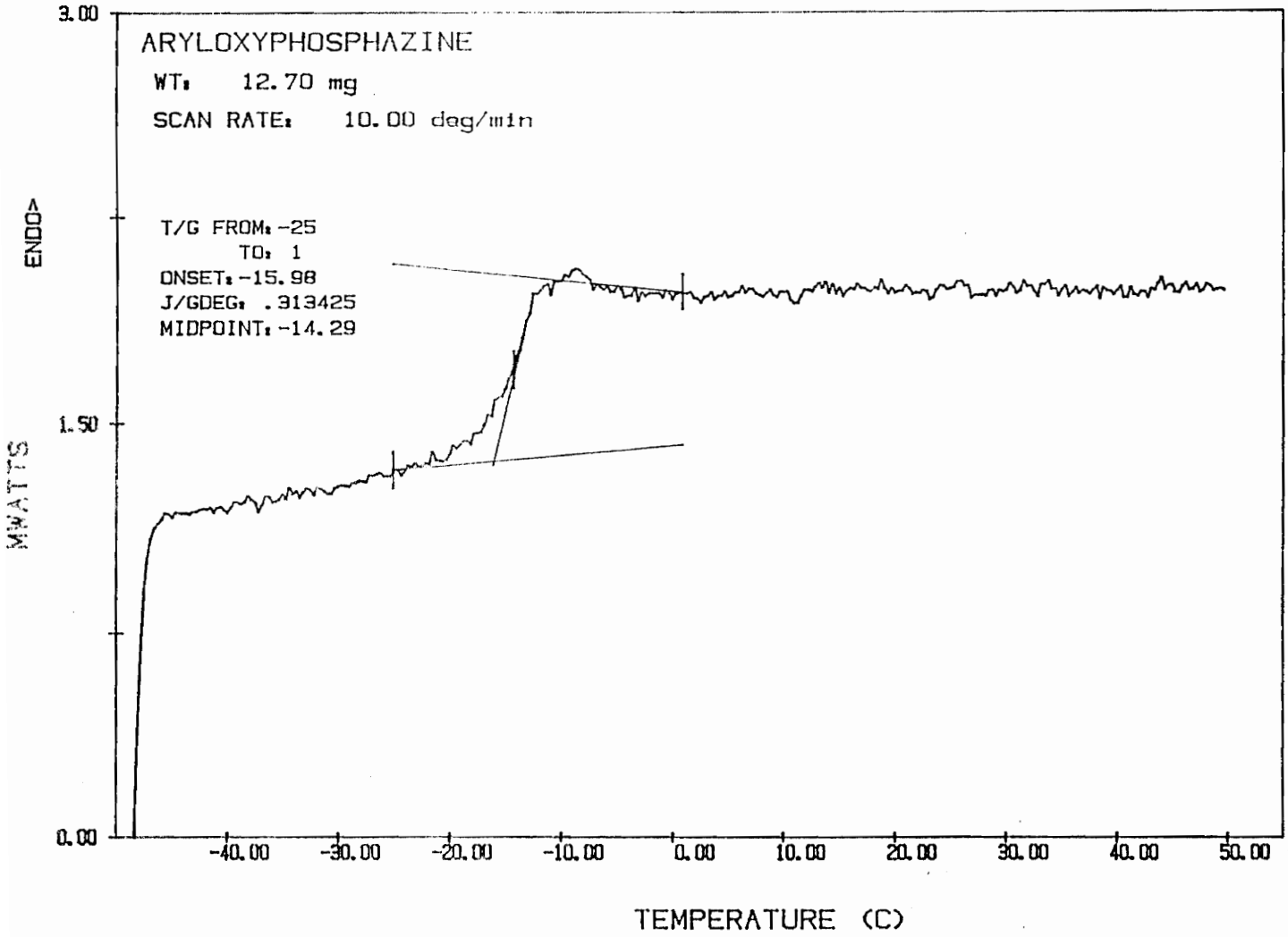

Figure 15.. Multiple frequency spectra Tan δ Vs temperature

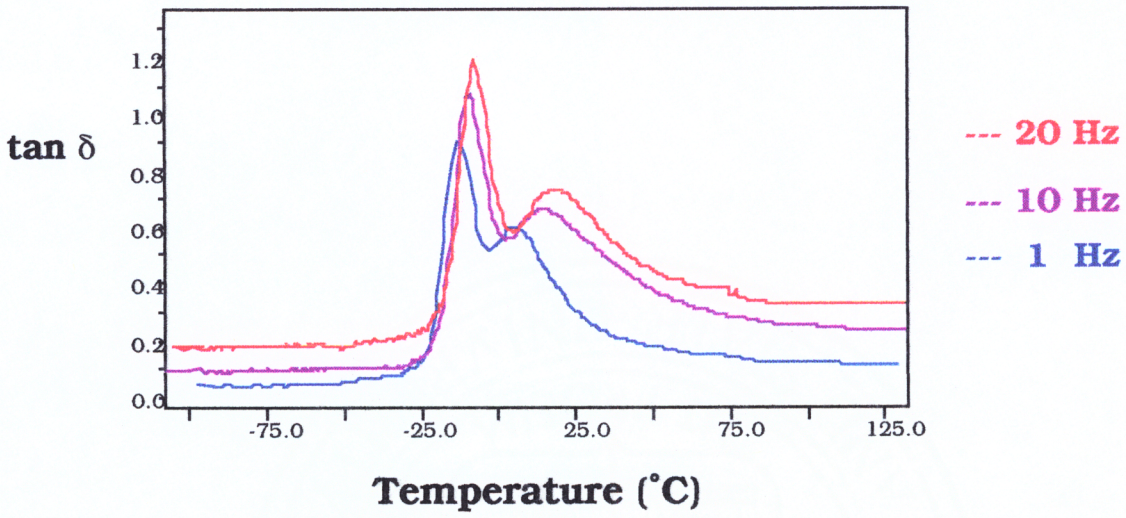

allows for variations in the application temperature depending upon the specific use the manufacturer may have. This reliance of the molecular dispersions on frequency allows one to determine the energy needed to initiate cooperative molecular motions in the material. The activation energies for each of the peaks were determined through a variation of the Arrhenius equation shown below in which ω is defined as the frequency.

$$\omega = \omega_0 \exp(-\Delta H/RT)$$

$$\log \omega = \log \omega_0 - 2.303(\Delta H/RT)$$

By plotting logarithm of the test frequencies versus the reciprocal of the absolute temperature, the activation energy is proportional to the slope of these plots. Figure 15 shows both of these activation energy plots. The calculated energies were 51.8 and 31.1 kJ/mol for the first and second relaxations, respectively. These computed values were slightly less than anticipated since the activation energies relating to micro-Brownian motions typically possess magnitudes of 100 kJ/mol or greater. This deviation arises from the lack of barriers for torsional rotations in the polymer backbone of this particular class of polymeric materials. As mentioned in section 2.3.1, the lone electron on nitrogen can be projected onto any of the 3d orbitals of phosphorus. The outcome is minimal opposition to main chain rotation and decreased activation energies when compared to open ended conjugated carbon chains. Comparison of the glass transition of similar carbon based materials provides further evidence to support this conclusion. These polymers typically possess glass transitions in excess of 100°C resulting from the additional thermal energy essential to initiate cooperative molecular motions. Dynamic mechanical experiments demonstrate the exceptional vibrational damping capabilities that this copolymer of polyphenoxy-ethylphenoxyphosphazene and polydiphenoxyphosphazene possess and their frequency dependence. These qualities are essential for successful sealant application. The lower temperature limit for application for the blended material was established to be -10°C.

Figure 16 Activation energy plot for α transitions the1st peak A) and the latter second peak B).

A)

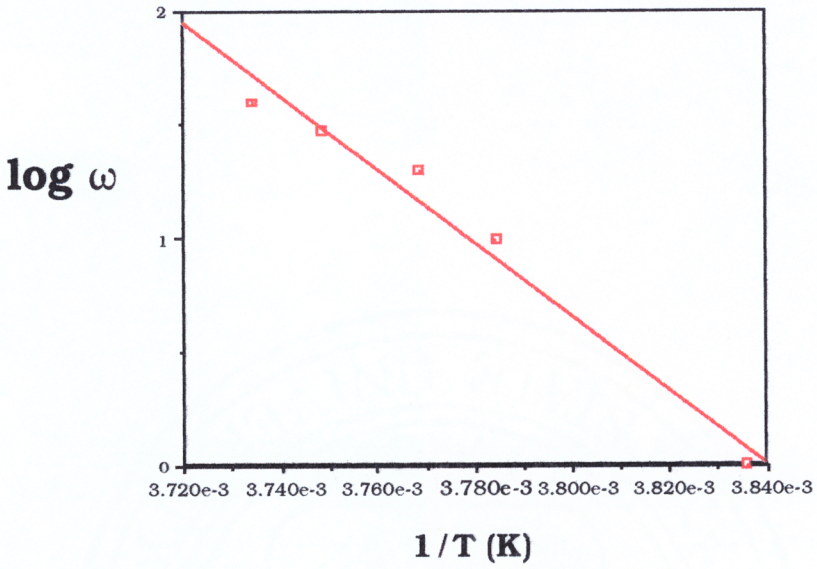

B)

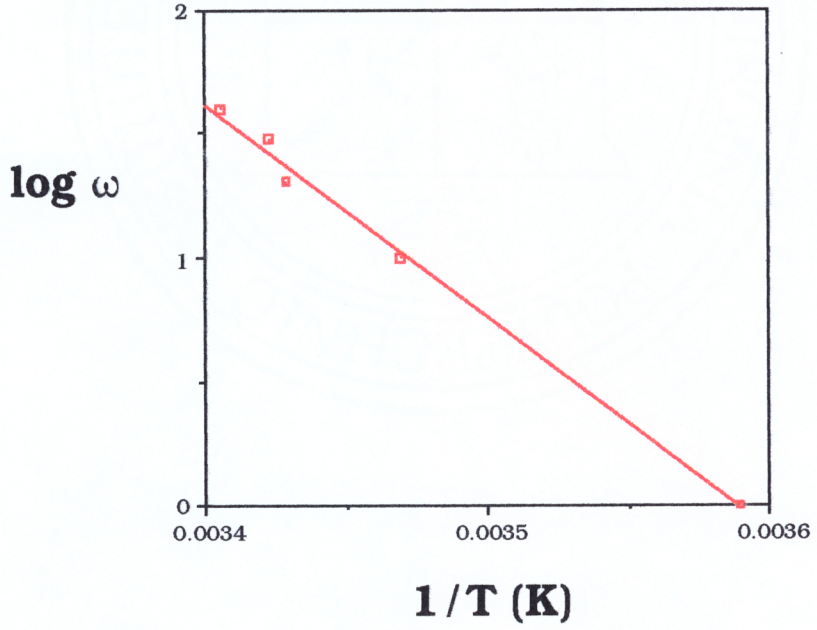

8.0 Conclusions

The focus of this research was to examine polyphenoxy-ethylphenoxyphosphazene, to access a few of its bulk properties, and predict favorable sealant conditions and usage. Sealants are defined as low strength flexible materials that provide barriers to the passage of vapors, gases, liquids, or solids. Typically sealants possess: an initial storage modulus less than 10^9 Pa, vibrational damping abilities, solvent resistance, and thermal stability. These physical criteria were investigated through solution, thermal stability, and dynamic mechanical experimentation.

Initial solvent ingression experiments revealed that Fedors' group contribution tables were applicable only as crude estimations of the solubility parameter. Experimental results illustrated that the solubility parameter and solvent - polymer interactions are affected by polar forces, hydrogen bonding, and london dispersive forces. Solvent - polymer interactions were at their greatest in solvents that possessed low polar and hydrogen bonding contributions of the solubility parameter. Therefore, favorable sealant applications of polyphenoxy-ethylphenoxyphosphazene are feasible in highly polar and hydrogen bonding environments, where solvent resistance is at a maximum.

Thermal profiles created from the thermogravimetric analysis of polyphenoxy-ethylphenoxyphosphazene resembled the work previously done by Allcock and others. Upon heating, the material undergoes chain cleavage and depolymerization to cyclic and oligomeric species subsequent

crosslinking reactions of the cyclic species to form a network structure. With this in mind, the upper temperature limit of application should not exceed 200°C even though the apparent thermal stability surpasses 400°C. Kinetic evaluation illustrated that thermal degradation mechanisms are dependent upon atmospheric conditions. Thermal profiles in air and nitrogen produced contrasting results. Nitrogen atmospheres displayed degradative behavior that followed simple kinetic equations while more complex kinetics occurred in air environments.

Dynamic mechanical experiments uncovered two prominent relaxations in the tan δ spectrum. The multiple peaks indicate the presence of two phases. Poor control of the synthetic variables during the substitution reaction may have resulted in the formation of a copolymer. The formation of this copolymeric material may have been a deliberate act by the manufacturer. This phase separated material may be composed of polyphenoxy-ethylphenoxy-phosphazene and polydiphenoxyphosphazene. Each of the dispersions are associated with the glass transition of its respective material. The emergence of two distinct phases increases the vibrational damping abilities in two ways. First, the measure of vibrational damping abilities of a material is proportional to the area under the α transition curve in the tan δ spectra. By having two separate phases, the area under this tan δ curve doubled. Secondly, the presence of the additional phase also increases the temperature range over which these vibrational damping qualities occur. These vibrational damping qualities are essential for sealant application. The lower temperature limit of application should not fall below -16°C, the glass transition of the polyphenoxy-ethylphenoxy-phosphazene phase. The initial storage modulus was found to be less than 10^9 Pa, one of the physical

requirements of a sealant material, and upon passage through the glass transition a rubbery plateau is reached that is characteristic of a crosslinked material. Repeated dynamic mechanical experiments at different frequencies illustrate that the vibrational damping qualities of this material depend upon the frequency as well as temperature. Activation energies determined for each of the α transitions based upon the multi frequency experiments were found to be lower than expected. These diminished activation energies relate to polyphosphazenes flexible polymer structure as a consequence of the materials lack of barriers to torsional rotation.

Based upon these results, the copolymeric polyaryloxyphosphazene displayed bulk properties ideal for sealant applications under these conducive conditions. Sealant use is most favorable in environments that promote interactions with highly polar or hydrogen bonding solvents. Minimal polymer- solvent interactions occur under these conditions, a trait desirable for successful sealant operations. The temperature application window for the copolymer of polyphenoxy-ethylphenoxyphosphazene and diphenoxyphosphazene ranges from -20 - 200°C. The upper temperature limit of application is associated with the thermal stability of the material while the lower is related to the glass transition and vibrational damping abilities of the polyphenoxy-ethylphenoxyphosphazene. The lower temperature limit is subject to frequency effects and the use temperature may shift depending on the application, allowing for a variety of practices.

9.0 References

1. R. W. Allen and H. R. Allcock, *Macro..*, 9, 956, (1976).
2. H. R. Allcock, M. S. Connolly, J. T. Sisko, and S. Al-Shai, *Macro.*, 21, 323, (1988).
3. Ph. Potin, *Eur. Polym. J.*, 27, #4-5, 341, (1991).
4. J. Wohler, *Anna. Chem.*, 11, 139, (1834).
5. H. Rose, *Anna. Chem.*, 11, 131, (1834).
6. N. S. Stokes, *Am. Chem. J.*, 19, 792, (1897).
7. H. R. Allcock and R. L. Kugel, *J. Am. Chem. Soc.*, 87, 4216 (1965).
8. E. D. Hornbaker and H. M. Li, U. S. Patent 4 198 381, (1980).
9. M. Heloui, R. De Jaegar, E. Puskaric, and J. Heubel, *Makromol. Chem.*, 183, 113, (1986).
10. R. Singler, N. Schneider, and G. Hagnauer, *Poly. Eng. and Sci.*, 15 #5, 321, (1975).
11. H. R. Allcock, R. L. Kugel, and K. J. Valan, *Inorg. Chem.* , 5, 1709, (1966).
12. R. Singler, N. Schneider, G. Hagnauer, B. R. LaLiberte, R. E. Sacher, and R. W. Matton, *J. Polym. Sci., Polym. Chem*, 12, 433, (1974).
13. G. Allen, C. J. Lewis, and S. M. Todd, *Polymer*, 11, 31, (1970).
14. H. R. Allcock and R. L. Kugel, *Inorg. Chem.*, 5, 1716, (1966).
15. H. R. Allcock and T. L. Evans, *J. Macromole. Sci. Chem.*, A16, 409, (1981).
16. H. R. Allcock and R. J. Best, *Can. J. Chem.*, 42, 447, (1965).
17. H. H. Sisler, S. E. Frazier, R. G. Rice, and M. G. Sanchez, *Inorg. Chem.*, 5, 326, (1966).
18. J. E. Mark, H. R. Allcock, and R. West, *Inorganic Polymers Ch. 3*, Prentice Hall Publishing New Jersey, (1992).
19. R. W. Allen and H. R. Allcock, *Macro.*, 9, 956, (1976).
20. J. MacCallum and J. Tanner, *J. Macromol. Sci.*, A4(2), 481, (1970)
21. H. R. Allcock, W. J. Cook, and D. Mack, *Inorg. Chem.*, 11, 2584, (1972).
22. F. Patat and K. Frombling, *Monatsh Chem.*, 86, 718, (1955).
23 H. R. Allcock, R. L. Kugel, and K. J. Valan, *Inorg. Chem.* , 5, 1709, (1966).
24. H. R. Allcock, G. Y. Moore, and W. J. Cook, *Macro*, 7, 571, (1974).
25. H. R. Allcock and W. J. Cook, *Macro*, 7, 284, (1974).
26. H. R. Allcock, G. S. McDonnell, G. H. Riding, and I. Manners, *Chem Mater.*, *2*, 425 (1990).
27. G. L. Hagnauer and N. S. Schneider, *J. of Polym. Sci*, 10 A-2, 699, (1972).

28. R. S. Schneider and R. E. Singler, *U.S. Army Materials and Mechanics Research Center*, unpublished work.
29. T. M. Connelly Jr. and J. K. Gilham, *Am. Chem. Soc. Polym. Prepr.*, 15 #2, 458 (1974).
30. D. W. Van Krevelen and J. Hoftyzer, *Properties of Polymer; Their Estimation and Correlation with Chemical Structure*, Elsevier Scientific Publishing, New York, (1976).
31. J. H. Hildebrand, *J. Am. Chem. Soc.*, 38, 1452, (1916).
32. G. Scatchard, *Chem. Revs.*, 8, 321, (1931).
33. J. H. Hildebrand, and R. L. Scott, *The Solubility of Non-Electrolytes*, Reinhold Publishing, (1949).
34. M. Dunkel, *Z. Physik. Chem*, A138, 42, (1928).
35. R. A. Hayes, *J. Appl. Polym. Sci.*, 5, 318, (1961).
36. A. T. Di Benedetto, *J. Polym. Sci.*, A1, 3459, (1963).
37. A. E. Rheineck and K. F. Lin, *J. Paint Technol.*, 40, 611, (1968).
38. D. W. Van Krevelen and J. Hoftyzer, *J. Appl. Polym. Sci.*, 11, p2189, (1967).
39. R. F. Fedors, *Polym. Eng. Sci.*, 14, 147, (1974).
40. C. M. Hansen, *Ind. Eng. Chem. Prod. Res. Dev.*, 8, 2, (1969).
41. E. B. Bagley, T. Nelson, and J. M. Scigliano, *J. Paint Technol.*, 43, 35, (1971).
42. T. Murayama, *Encylopedia of Polym. Sci. and Eng.*, 5, 299, (1981).
43. N. G. McCrum, B. E. Read, and G. Williams, *Anlastic and Dielectric Effects in Polymeric Solids*, Dover Publications, New York, (1967).
44. J. D. Ferry, *Viscoelastic Properties of Polymers*, 3rd ed., John Wiley and Sons, New York, (1980)
45. K. Deutsch, E. A. Hoff, abd W. Reddish, *J. Polym. Sci.*, 13, 565, (1954).
46. E. Helfand, *Rubber Chem. Technol.*, 36, 1303, (1963).
47. E. A. Sidorovitch, A. I. Marei, N. S. Gashto'd, *Rubber Chem. Technol.*, 44, ,166, (1971).
48. J. H. Flynn, *Encylopedia of Polym. Sci. and Eng.*, Supplement, 690, (1984).
49. H. L. Friedman, *J. Polym. Sci.*, 50, 183, (1965).
50. T. Ozawa, *Bull. Chem. Soc. Japan*, 38, 1881, (1965).
51. J. H. Flynn and L. A. Wall, *Polym. Lett.*, 4, 191, (1966).
52. J. H. Flynn, *J. of Therm. Analy.*, 27, 95, (1983).